

**AUTOMATED DETECTION AND ANALYSIS
OF SPEED LIMIT SIGNS**

Final Report
FEBRUARY 2002

Bahram Javidi
Maria-Albertina Castro
Sherif Kishk
Elisabet Pérez

JHR 02-285

Project 00-4

This research was sponsored by the Joint Highway Research Advisory Council (JHRAC) of the University of Connecticut and the Connecticut Department of Transportation and was carried out at the Connecticut Transportation Institute of the University of Connecticut.

The contents of this report reflect the views of the authors who are responsible for the facts and accuracy of the data presented herein. The contents do not necessarily reflect the official views or policies of the University of Connecticut or the Connecticut Department of Transportation. This report does not constitute a standard, specification, or regulation.

Technical Report Documentation Page

1. Report No. JHR 02-285	2. Government Accession No. N/A	3. Recipient's Catalog No. N/A	
4. Title and Subtitle AUTOMATED DETECTION AND ANALYSIS SPEED LIMIT SIGNS		5. Report Date February 2002	
		6. Performing Organization Code N/A	
7. Author(s) Bahram Javidi, Maria-Albertina Castro, Sherif Kishk, Elisabet Pérez		8. Performing Organization Report No. JHR 02-285	
9. Performing Organization Name and Address University of Connecticut Connecticut Transportation Institute Storrs, CT 06269-5202		10. Work Unit No. (TRAIS) N/A	
		11. Contract or Grant No. N/A	
12. Sponsoring Agency Name and Address Connecticut Department of Transportation 280 West Street Rocky Hill, CT 06067-0207		13. Type of Report and Period Covered FINAL	
		14. Sponsoring Agency Code N/A	
15. Supplementary Notes N/A			
16. Abstract Design of an on-board processor that enables recognition of a given road sign affected by different distortions is studied. The road sign recognition system is based on a nonlinear processor. Analysis of different filtering methods allows us to select the best techniques to overcome a variety of distortions. The proposed recognition system has been tested in real still images as well as in video sequences. Scenes were captured in real environments, with cluttered backgrounds and contain many distortions simultaneously. Recognition results for various images show that the processor is able to properly detect a given road sign even if it is varying in scale, slightly tilted or viewed under different angles. Recognition is also achieved when dealing with partially occluded road signs. In addition, the system is robust to illumination fluctuations.			
17. Key Words Pattern Recognition, Distortion-Tolerant Processor, Road Sign Detection		18. Distribution Statement No restrictions. This document is available to the public through the National Technical Information Service Springfield, Virginia 22161	
19. Security Classif. (of this report) Unclassified	20. Security Classif. (of this page) Unclassified	21. No. of Pages 53	22. Price N/A

Acknowledgements

The authors are grateful to Richard C. Hanley of the Connecticut Department of Transportation, Division of Research, for his fruitful comments.

The authors also want to thank their students and collaborators Dr. Yann Frauel, for their support on this research.

Modern Metric Conversion Factors

SI* (MODERN METRIC) CONVERSION FACTORS

APPROXIMATE CONVERSIONS TO SI UNITS

Symbol	When You Know	Multiply By	To Find	Symbol	When You Know	Multiply By	To Find	Symbol
LENGTH								
in	inches	25.4	millimetres	mm	mm		inches	in
ft	feet	0.305	metres	m	m		feet	ft
yd	yards	0.914	metres	m	m		yards	yd
mi	miles	1.61	kilometres	km	km		miles	mi
AREA								
in ²	square inches	645.2	millimetres squared	mm ²	mm ²		square inches	in ²
ft ²	square feet	0.093	metres squared	m ²	m ²		square feet	ft ²
yd ²	square yards	0.836	metres squared	m ²	m ²		acres	ac
ac	acres	0.405	hectares	ha	ha		square metres	m ²
mi ²	square miles	2.59	kilometres squared	km ²	km ²			
VOLUME								
fl oz	fluid ounces	29.57	millilitres	mL	mL		fluid ounces	fl oz
gal	gallons	3.785	Litres	L	L		gallons	gal
ft ³	cubic feet	0.028	metres cubed	m ³	m ³		cubic feet	ft ³
yd ³	cubic yards	0.765	metres cubed	m ³	m ³		cubic yards	yd ³
NOTE: Volumes greater than 1000 L shall be shown in m³								
MASS								
oz	ounces	28.35	grams	g	g		ounces	oz
lb	pounds	0.454	kilograms	kg	kg		pounds	lb
T	short tons (2000 lb)	0.907	megagrams	Mg	Mg		short tons (2000 lb)	T
TEMPERATURE (exact)								
°F	Fahrenheit temperature	5(F-32)/9	Celsius temperature	°C	°C		Fahrenheit temperature	°F

°F	°C	°F	°C	°F	°C
-40	-40	32	0	212	100
0	-18	98.6	37	200	93.3
100	38				

* SI is the symbol for the International System of Measurement

Table of contents

Title page; Disclaimer.	i
Technical report documentation page	ii
Acknowledgements	iii
Modern metric conversion factors	iv
Table of contents	v
List of figures	vi
Symbols.	ix
1. Introduction	1
2. Principles of image processing based on pattern recognition	1
2.1 Linear processors	1
2.2 Nonlinear processors	2
2.3 Metrics for performance evaluation	3
3. Filtering techniques for distortion-tolerant systems	4
4. Scale-invariant road sign recognition system	5
4.1 Determination of nonlinearity strength	5
4.2 Composite nonlinear filters	7
4.3 Bank of single nonlinear filters	10
5. Rotation-tolerant road sign recognition system	12
5.1 Tolerance to out-of-plane rotations. Synthesis of composite nonlinear filters	12
5.2 Tolerance to in-plane rotations. Rotation of the input scene	12
5.3 Threshold determination	13
5.4 Recognition results for 35mph speed limit sign	14
6. Recognition system to detect all the speed limit signs	22
6.1 Recognition of speed limit signs regardless of their speed limit number	
Synthesis of composite nonlinear filters	22
6.2 Description of the entire proposed recognition system	23
6.3 Threshold determination	25
6.4 Recognition results	42
7. Analysis of a video sequence	42
8. Summary	42
References	44

List of Figures

Figure 1. Diagram of a nonlinear processor used to obtain the correlation between the scene to be analyzed and the reference target.

Figure 2. Diagram of the synthesis of a nonlinear composite filter.

Figure 3. a) Reference target; b) Training true target; f) False target, and d) Non-training true target.

Figure 4. Correlation planes for different nonlinearities. Planes on the left column correspond to the analysis of a true target. Planes on the right correspond to a false target.

Figure 5. PCE results for different nonlinearities. a) $k = 1$ (linear case); b) $k = 0.5$; c) $k = 0.1$ and e) $k = 0$ (binarizing nonlinearity).

Figure 6. Recognition results for the first nonlinear composite filter. a) Probability of error in the classification of training images. b) Classification of true targets and false targets with respect to the established threshold value. c) Correlation peak position versus the actual target position in the scene.

Figure 7. Recognition results for the second nonlinear nonlinear filter. a) Probability of error in the classification of training images. b) Classification of true targets and false targets with respect to the established threshold value. c) Correlation peak position versus the actual target position in the scene.

Figure 8. Recognition results for a bank of nonlinear single filters. a) Probability of error in the classification of training images. b) Classification of true targets and false targets with respect to the established threshold value. c) Correlation peak position versus the actual target position in the scene. d) maximum PCE value versus the distance between the detected road signs and the acquisition system

Figure 9. Recognition results for a bank of nonlinear single filters with an increase in the number of samples. a) Probability of error in the classification of training images. b) Classification of true targets and false targets with respect to the established threshold value. c) Correlation peak position versus the actual target position in the scene. d) maximum PCE value versus the distance between the detected road signs and the acquisition system

Figure 10. a) A nonlinear composite filter constructed from several out-of-plane rotated version of the 35mph speed limit sign, and b) bank of nonlinear composite filter.

Figure 11. Recognition system for the 35mph speed limit sign tolerant to in-plane and out-of-plane rotations as well as scale invariant and illumination invariant.

Figure 12. Determination of the threshold. A) Probability of error vs. the PCE of the correlation result, and b) PCE value for true targets and false targets.

Figure 13. Recognition of a true-training 35mph speed limit sign. a) Image containing a 35mph speed limit sign on a real background. b) Output correlation plane. c) Location of the detected target.

Figure 14. Recognition of training true-target for a non-training scale of the 35mph speed limit sign besides an object of similar shape. a) Analyzed scene. b) Output correlation plane. c) Location of the detected target.

Figure 15. Identification of a far and slightly in-plane rotated 35mph speed limit sign in the presence of another road sign. a) Analyzed scene. b) Output correlation plane. c) Location of the detected target.

Figure 16. Identification of a rotated 35mph speed limit sign. a) Analyzed scene. b) Output correlation plane. c) Location of the detected target.

Figure 17. Out-of-plane rotated 35mph speed limits sign. a) Analyzed scene. b) Output correlation plane. c) Location of the detected target.

Figure 18. Recognition of a rotated true-target under poor illumination. a) Analyzed scene. b) Output correlation plane. c) Location of the detected target.

Figure 19. Rejection of a false target. a) Analyzed scene. b) Output correlation plane.

Figure 20. Rejection of a false target road sign very similar in shape to the speed limits sign. a) Analyzed scene. b) Output correlation plane.

Figure 21. A nonlinear composite filter is built for comprising various speed limit signs with different speed limit number.

Figure 22. Recognition of all speed limit signs. System tolerant to in-plane rotations and scale-invariant. It is also robust to illumination fluctuations.

Figure 23. Determination of the threshold. a) Probability of error vs. the PCE of the correlation result; and b) PCE value for true targets and false targets.

Figure 24. Results for the same image as in figure 15, now using the filter bank of nonlinear filters that comprises all the speed limits.

Figure 25. Probability of error using cjl images. The set of images includes different rotated, scaled and non-uniform illuminated speed limit signs.

Figure 26. Threshold determination based on the “last opportunity detection” for cjl-format images.

Figure 27. Detection of a slightly rotated 30mph speed limit sign in the presence of an object of similar shape. a) Analyzed input scene. b) Output correlation plane. c) Location of the detected target.

Figure 28. Detection of a 30mph speed limit sign in the presence of objects with similar energy. a) Analyzed input scene. b) Output correlation plane. c) Location of the detected target.

Figure 29. Detection of a 35mph speed limit sign under poor illumination. a) Analyzed input scene, b) Output correlation plane. c) Location of the detected target.

Figure 30. Recognition of a partially occluded 50mph under poor illumination. a) Analyzed input scene. b) Output correlation plane. c) Location of the detected target.

Figure 31. Recognition of a 25mph speed limit sign under non-uniform illumination. a) Analyzed input scene. b) Output correlation plane. c) Location of the detected target.

Figure 32. Recognition of a far slightly rotated 45mph speed limit sign in the presence of another road sign. a) Analyzed input scene. b) Output correlation plane. c) Location of the detected target.

Figure 33. Recognition of a 40mph speed limit sign in the presence of a highly energetic demarcation line. a) Analyzed input scene. b) Output correlation plane. c) Location of the detected target.

Figure 34. Recognition of a rotated 35mph speed limit sign. a) Analyzed input scene. b) Output correlation plane. c) Location of the detected target.

Figure 35. Rejection of a far and non-uniform illuminated true target. The PCE of this correlation plane is lower than the pre-established threshold due to the small correlation peak in the true-position and a relative high noise due to other energetic objects. A closer recognized-image is presented in figure 31. a) Analyzed input scene. b) Output correlation plane. c) Location of the detected target.

Figure 36. Rejection of false targets. Several false road signs are present in the scene. a) Analyzed input scene, b) Output correlation plane.

Figure 37. Rejection of a false target of similar shape. a) Analyzed scene. b) Output correlation plane.

Figure 38. Rejection of a do not pass road sign. a) Analyzed scene. b) Output correlation plane.

Figure 39. Rejection of a false target. a) Analyzed scene. b) Output correlation plane.

Figure 40. Rejection of a false target. a) Analyzed scene. b) Output correlation plane.

Figure 41. Rejection of a false target. a) Analyzed scene. b) Output correlation plane.

Figure 42. Recognition results for the analysis of a video sequence.

Symbols

k	nonlinearity strength
PCE	peak-to-correlation energy parameter

1. INTRODUCTION

Development of safety systems is in increasing demand. These systems could be installed in vehicles to avoid accidents. A useful safety system should be able to recognize different objects, for instance road signs, and send the appropriate directions to the vehicle in order to react according to the information of the sign. That means, if a speed limit sign is detected, the vehicle should slow down and adjust to a proper speed. To properly detect road signs from a vehicle in motion, recognition system needs different requirements, such as scale-invariance, tolerance to changes in illumination, and robustness to background noise.

Different contributions have been proposed for distortion-invariant systems in the field of pattern recognition and image analysis. One of the most used techniques is the synthesis of composite filters, also called synthetic discriminant functions (SDF). They have been first introduced by Caulfield and Maloney^{1,2} and developed by the group of Casasent.^{3,4} Since then, other proposals of this category of filters have been made. For instance, minimum average correlation energy (MACE) filters are composite filters that improve the detection of the target by minimizing the average correlation plane energy.⁵ The aforementioned composite filters^{3,5} have their equivalent for a nonlinear processor. A rotation-invariant system has been achieved by the use of these synthetic discriminant functions in a nonlinear joint transform correlator.^{6,7} Nonlinear processors have been also studied in the case of a illuminant-invariant system.⁸ Design for a recognition system tolerant to various distortions has been also proposed⁹, and special attention has been paid to distortion-invariant systems under noisy environments.¹⁰⁻¹³

Pattern recognition techniques that deal with different types of distortions have been also introduced for a road sign recognition system. An optical processor for scale-invariant road sign detection was proposed^{14,15} partially invariant filters were applied in a processor based on multiple correlations to obtain road sign recognition with partial tolerance to in-plane rotations and scale-invariance.^{16,17}

The goal of this work is to develop a recognition system that enables automatic recognition of road signs. We will focus our attention to a scale, rotation and illumination-invariant pattern recognition system. And we will analyze scenes captured in a real background noise. This system will be based on a nonlinear processor, which performs several nonlinear correlations between an input scene and different reference targets. A bank of nonlinear single filters will store the information of the reference varying in scale. The applied nonlinearity will provide the system with illumination invariance. Rotation of the input signal allows tolerance to in-plane rotations, and finally, composite filters are designed to achieve tolerance to a given information of the sought road sign.

2. PRINCIPLES OF IMAGE PROCESSORS BASED ON PATTERN RECOGNITION

2.1. Linear processors

One of the most widespread techniques used in pattern recognition is based on the correlation between the scene to be analyzed, $s(x, y)$, and the reference target to be detected, $r(x, y)$. The mathematical expression for correlation is defined by^{18,19}

$$c(x, y) = s(x, y) \otimes r(x, y) = \int_{-\infty}^{\infty} \int_{-\infty}^{\infty} s(\xi, \eta) r^*(\xi - x, \eta - y) d\xi d\eta, \quad (1)$$

where $*$ denotes complex conjugate and \otimes correlation. This function measures similarity between two objects. Not only does correlation detect the presence of an object, but also it determines its position in the scene. If there is a good match between an object of the scene and the reference target, a high peak appears in the correlation plane $c(x, y)$ at the location of the object in the scene. Height of the peak, as well as its sharpness depends, among others, on the degree of similarity between the two correlated functions.

Correlation can be also expressed in terms of Fourier transforms. Let $\hat{s}(\mu, \nu)$ and $\hat{r}(\mu, \nu)$ be the Fourier transforms of $s(x, y)$ and $r(x, y)$, respectively, where the Fourier transform of a function is defined by^{18,19}

$$\hat{s}(\mu, \nu) = TF\{s(x, y)\} = \int_{-\infty}^{\infty} \int_{-\infty}^{\infty} s(\xi, \mu) \exp[-i2\pi(\mu\xi + \nu\eta)] d\xi d\eta. \quad (2)$$

Correlation between two functions satisfies^{18,19}

$$c(x, y) = TF^{-1}\{\hat{s}(\mu, \nu) \hat{r}^*(\mu, \nu)\} \quad (3)$$

where TF^{-1} stands for the inverse Fourier transform. Equation (3) shows that correlation between two functions can be obtained by multiplying their Fourier transforms in the frequency domain followed by inverse Fourier transforming the resulting distribution. Since Fourier transform and product operations can be achieved optically, correlation between two functions can also be implemented optically. Systems that perform correlation are named correlators and they permit real-time processing of a large amount of information using optics. The combination of advantages given by optics, along with some properties provided by electronics has made feasible the implementation of powerful hybrid opto-electronic processors for solving different pattern recognition tasks.

2.2. Nonlinear processors

The beginning of image analysis based on pattern recognition can be placed in 1964 when Vander Lugt proposed a spatial matched filtering method.²⁰ Since then, techniques, architectures and algorithms have been developed and improved to obtain more versatile and efficient recognition systems. Linear correlators described by Eq. (1) have many limitations for recognizing objects in background noise.²¹⁻²⁵ In addition, these correlators are not tolerant of image distortions such as rotation, scale and illumination fluctuations. Image processing and spatial filtering techniques have been proposed to remedy these problems.¹⁻¹³

Applying different spatial filtering techniques prior to multiplying their Fourier transforms in the frequency domain can modify information of the scene to be analyzed as well as information of the target. Selected information of the objects to be correlated can be enhanced or modified depending on the recognition task to be solved. Some filtering techniques are set to detect an object depending on a given feature such as contour, color, and texture. As it was already mentioned, sometimes it is necessary to recognize an object that presents some distortion such as scale variation or rotation.¹⁻⁹ Or even to detect an object when the signal is degraded by noise.¹⁰⁻¹³

When a nonlinear operator modifies the Fourier transforms of both, the scene and the target, then we consider the processor to be a nonlinear correlator.²⁶ As an example, operations performed in a nonlinear correlator to obtain the output plane of the recognition system are shown in the diagram of figure 1.

Nonlinear filtering is being used in this work due to its superior performance in comparison with linear filtering techniques in terms of discrimination capability, correlation peak sharpness, and noise robustness.^{26,27} In a k 'th-law nonlinear processor,²⁶ the nonlinear operator applied symmetrically to the scene and the reference Fourier transforms.

Parameter k controls the strength of the nonlinearity. It includes all the degrees from linear filtering techniques ($k=1$) to binarizing nonlinearities ($k=0$). Intermediate values of k permit to vary the features of the processor, such as its discrimination capabilities or its illumination-invariance. Subsection 4.1 of this work shows the results that permit to choose an appropriate value of parameter k for the following experiments.

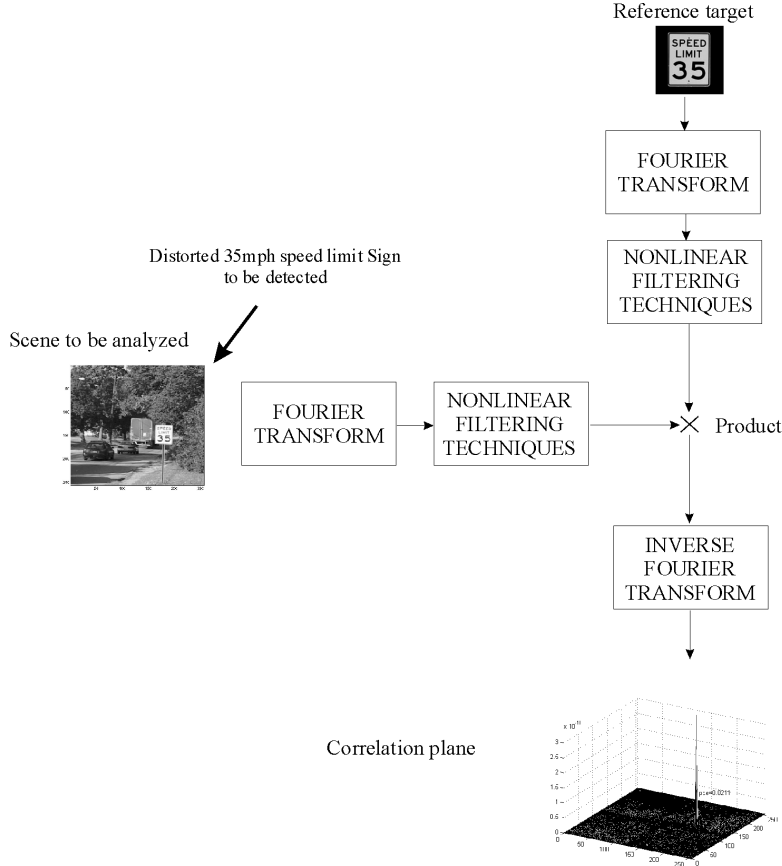


Figure 1. Diagram of a nonlinear processor used to obtain the correlation between the scene to be analyzed and the reference target.

2.3. Metrics for performance evaluation

There exist many different metrics to evaluate correlation filter performance. Some of them are described in summarizing works elsewhere.²⁷ To evaluate correlation results in our experiments we will use a criterion based on the peak-to-correlation energy (PCE) parameter, which is defined²⁷

$$PCE = \frac{|c(0,0)|^2}{\iint |c(x,y)|^2 dx dy}. \quad (4)$$

This parameter measures the ratio between the intensity value of the output peak at the target location and the total energy of the output plane. In general, a high and sharp correlation peak is expected when there is an object in the scene that matches the reference target, thus leading to a high value for the PCE parameter. A better match between an object of the scene and the reference, a closer value to unity for the PCE parameter will be reached.

As the proposed recognition system performs multiple correlations between the scene and a set of reference targets, the final recognition result is based on a winner-take-all model. The PCE parameter is computed for all the output planes, and the output plane with the maximum PCE value is selected as the final response of the system.

A threshold operation that permits to accept a true target or to reject a false object is established by means of a learning algorithm. A set of training images, containing true road sign targets and false signs, is needed to establish the appropriate threshold value for the output of the recognition system.

PCE values above the threshold will indicate that an object in the scene is recognized as similar to the target. Conversely, PCE values below the threshold will imply the rejection of the object.

3. FILTERING TECHNIQUES FOR DISTORTION-TOLERANT SYSTEMS

Different approaches to obtain distortion-tolerant recognition systems exist. They have in common the need of storing information of the object to be recognized taking into account different distortions that can affect the reference.

The most straightforward way to keep the information of the distorted versions of a target is to design a single filter for each type of distortion to be considered. In this case, we will talk of a filter bank. To determine if a target, distorted or not, is present in a given scene, it will be necessary to correlate or compare the scene with the multiple filters belonging to the bank. This technique could be time-consuming and it is sometimes overcome by the use of composite filters.

In a general approach, the information included in a composite filter consists of various views of the target under different situations (different rotation angles, scale variations, changes in illumination, etc.). Taking into account different constraints carries out the synthesis of all the information in a unique composite filter. The constraint operations provide desirable features of the composite filter such as sharp correlations peaks, noise robustness, low output-noise floor, etc. A scheme of the operations performed to synthesize a nonlinear composite filter tolerant to scale-variations of the object is shown in figure 2, where a nonlinear composite filter was built considering several scales of a particular speed limit sign.

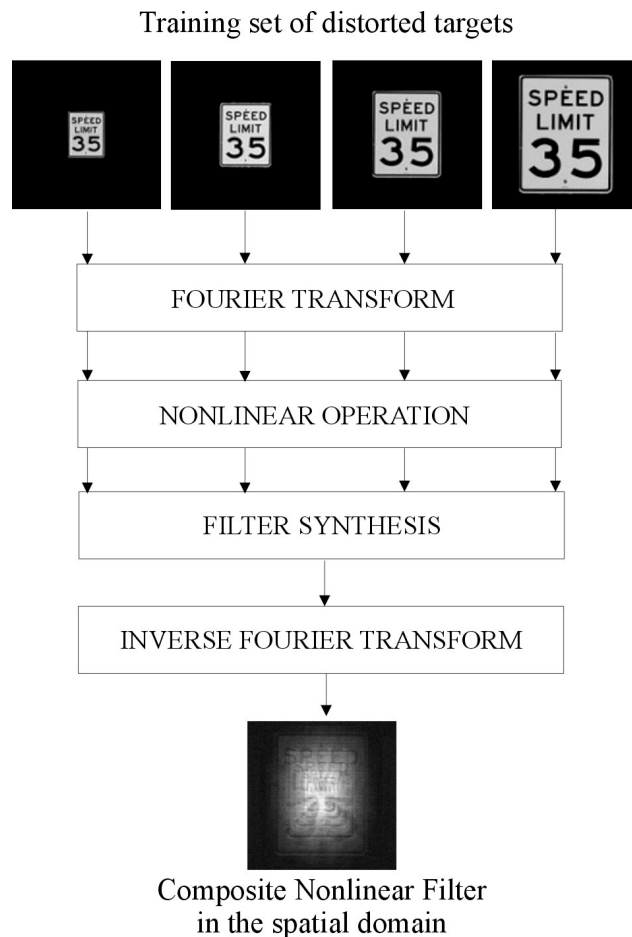


Figure 2. Diagram of the synthesis of a nonlinear composite filter.

The principal advantage of a composite filter in front of a bank of single filters is the reduction of time in the processing step. Only a single correlation can be enough to compare a given image with the whole set of distorted versions of the sought target. However, composite filters can lack of noise robustness and discrimination capability. In a composite filter, the number of images (distorted versions) of the reference is limited in order to obtain a satisfactory performance.

In this work, Fourier-plane nonlinear filters^{6,7} are used as composite nonlinear filters. They are modifications of other well-known distortion-invariant filters.^{3,5} It has been shown that Fourier-plane nonlinear filters have tolerance to in-plane and out-of-plane rotation, as well as, a good performance in the presence of different types of noise.^{6,7} Two different types of Fourier plane nonlinear filters will be tested in the following simulation experiments to design the recognition system.

4. SCALE-INVARIANT ROAD SIGN RECOGNITION SYSTEM

To test the tolerance of the system to variations in scale, an on-board camera has captured several images from different distances in a real environment. Speed limit signs are being used as true targets to be detected. Pictures containing speed limits have been captured in increments of uniform variation in scale. The closest road sign is 6 times larger than the farthest. This set of true targets images trains the recognition system, and is also used as the reference targets. Figure 3a shows one of the reference targets extracted from a training image containing a true target (Figure 3b).

Another set of images containing different road signs (false objects) is used to train the system and to evaluate its discrimination capabilities. The same procedure is used to capture several images in increments of uniform variation in scale. These pictures are also included in the training set. Figure 3c shows an example of false sign.

A different set of speed limit sign images is used as non-training targets to test the recognition system. The variation in scale of the non-training images is non-uniform. A sample of these images is shown in figure 3d.



Figure 3. a) Reference target; b) Training true target; c) False target, and d) Non-training true target.

The normalized images are Fourier transformed and the k 'th-law nonlinearity is applied to them. In all the cases, the nonlinear correlation output is obtained by taking the inverse Fourier transform of the product between the nonlinearly modified spectra of both the input signal and the reference target. Sometimes, the reference target will be a composite nonlinear filter. The complete correlation process was carried out digitally and results presented in the following sections were obtained by using the software Matlab 5.3 on a PC Pentium II at 400 MHz.

4.1. Determination of nonlinearity strength

We carry out a preliminary analysis in order to determine the nonlinearity that provides better recognition results for a particular road sign. For this reason, we perform by simulation the correlation of all the training images with the reference patterns. We obtain a correlation output for each pair of images captured at the same distance. The training set consists of 11 true target images and 11 false targets. Figures 4 and 5 show the obtained results for different values of k . Analysis from the linear

case ($k=1$) to a binarizing nonlinearity ($k=0$) is provided taking also into account intermediate values of the parameter k .

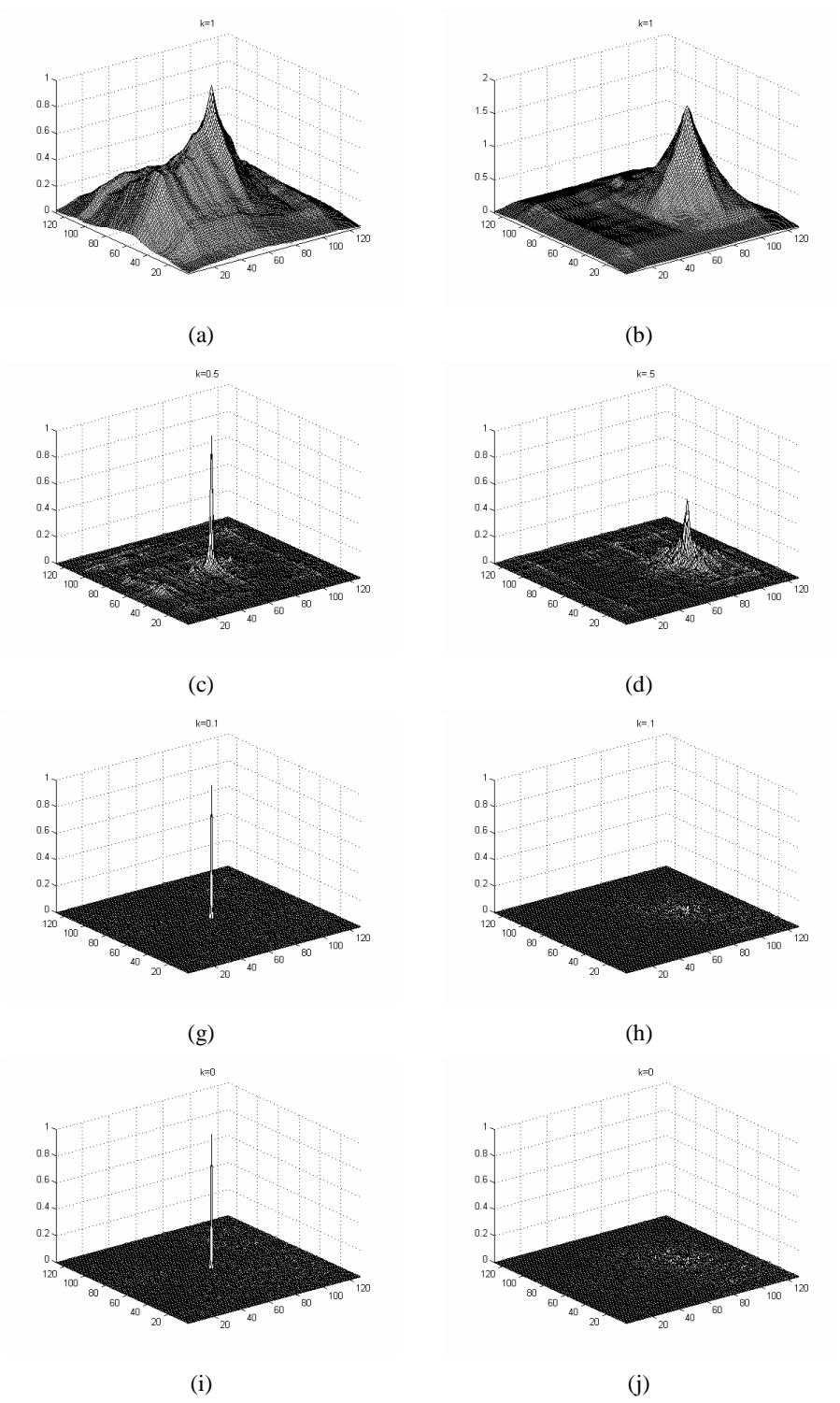


Figure 4. Correlation planes for different nonlinearities. Planes on the left column correspond to the analysis of a true target. Planes on the right correspond to a false target.

Output planes for different values of k are shown in figure 4. For a given true target correlation planes are displayed on the left column. Output planes shown on the right column correspond to a given false target. From figure 4 we observe that the highest peak on the lowest output-noise floor is achieved for $k=0.1$ (Figure 4g). A good discrimination for the false target is also obtained (Figure 4h).

In figure 5, we represent PCE values obtained for each image in the training set. We observe that the largest differences between PCE values of true targets and PCE values of false targets are achieved for low values of the parameter k .

In particular, our analysis showed that a nonlinearity of $k=0.1$ improves the correlation results in terms of peak sharpness and discrimination capability of the system. These results are in accordance with other results obtained for tolerance to target rotations.^{6,7}

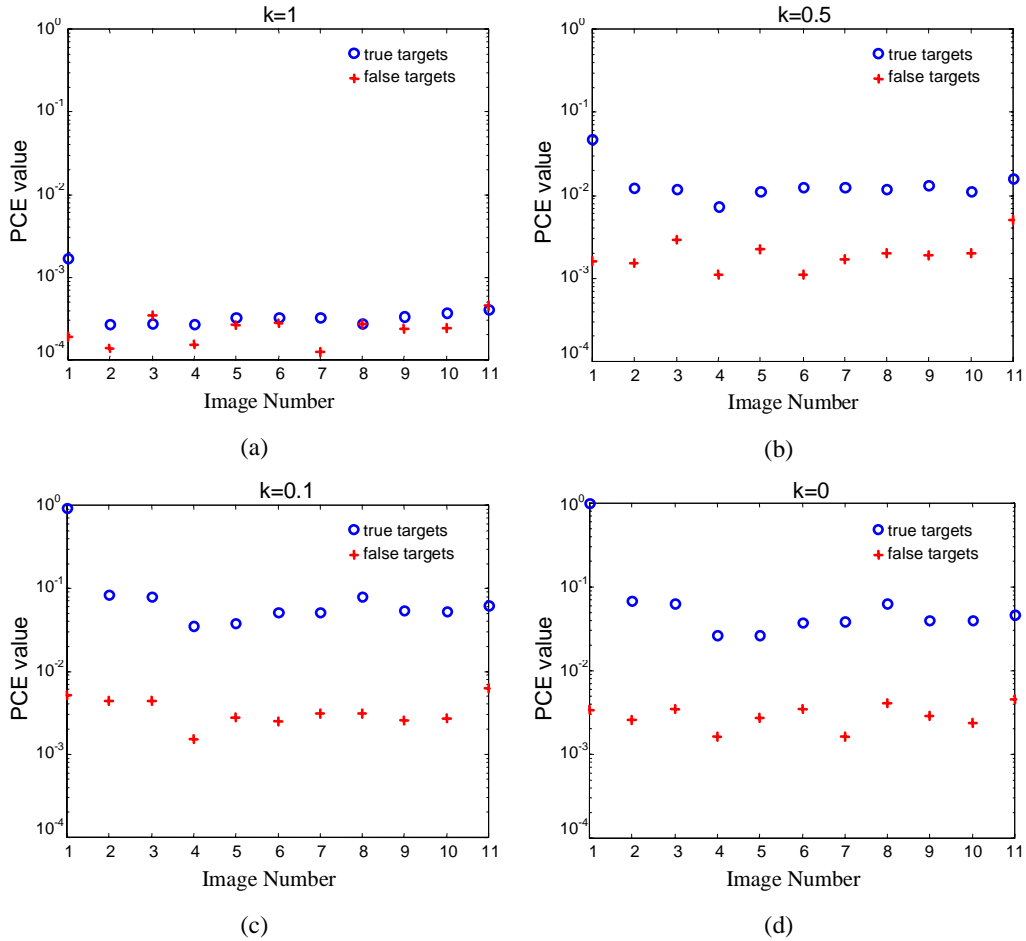


Figure 5. PCE results for different nonlinearities. a) $k = 1$ (linear case); b) $k = 0.5$; c) $k = 0.1$ and d) $k = 0$ (binarizing nonlinearity).

4.2. Composite nonlinear filters

We are interested in comparing the system's tolerance to scale variations of the target to be detected, by using two different methods: first, the design of composite nonlinear filters (subsection 4.2), and secondly, when a bank of single nonlinear filters is considered (subsection 4.3).

For the case of composite nonlinear filters, two types of filters are sequentially used in the recognition system. Their performance is evaluated and compared.

In the design of composite nonlinear filters, the 11 true target images of the training set are distributed in two groups. Each group is used to construct a composite nonlinear filter. Limiting the number of images per composite filter improves its performance in the recognition system. Thus, each composite filter has information of the true target varying in scale and captured from different range of distances. Parameter $k=0.1$ is used to implement both nonlinear composite filters.

For both types of composite nonlinear filters, recognition results are obtained for the entire training set, which is composed of true targets and false targets. The maximum PCE value is considered to classify signs as similar to the target or to discriminate them from the sign to be recognized. The training process allows selection of an appropriate threshold value for the output of the system. Output values above the threshold correspond to objects considered as true targets, whereas output values below the threshold imply the rejection of the object in the recognition process.

Figure 6a shows the probability of error in the recognition of a specific road sign, for the training set using the first nonlinear composite filter. A solid line in the graphs indicates the probability of error in classification of training signs. A dashed line plots probability of error in rejection of false targets. A minimum threshold value can be established when the probability of misclassification of false targets reaches the value of zero.

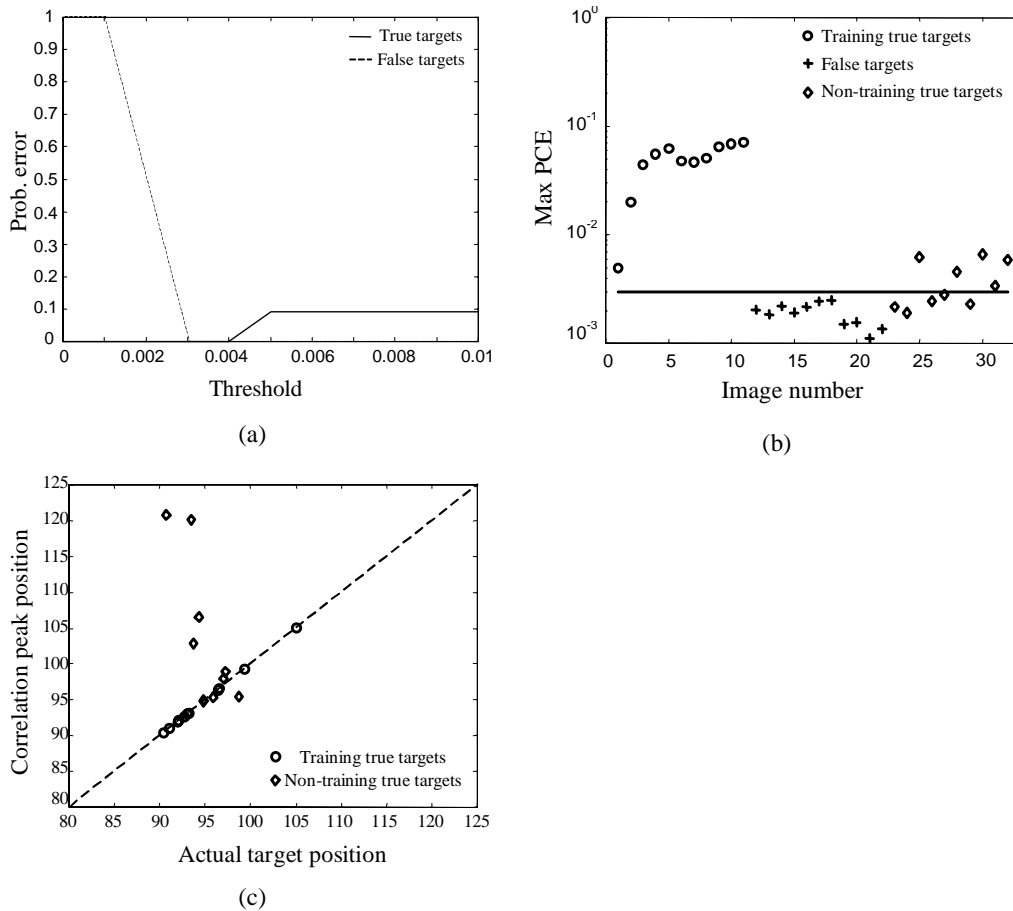


Figure 6. Recognition results for the first nonlinear composite filter. a) Probability of error in the classification of training images. b) Classification of true targets and false targets with respect to the established threshold value. c) Correlation peak position versus the actual target position in the scene.

Once the threshold is established, we use the entire set of images to test the performance of the system. Results for nonlinear composite filters are summarized in figure 6b. In this graph, the output response of the system is displayed. The maximum peak-to-correlation energy (PCE) values achieved among the different output planes are plotted for all the images. A horizontal solid line shows the chosen threshold level.

The maximum PCE value for non-training signs is above the threshold level in some cases. Thus, they are correctly recognized as the true class target. However, when the road sign is located at a far distance from the acquisition system, the processor is not able to properly detect the road sign due to the low resolution and energy of the target.

Figure 6c shows the position of the maximum correlation peak versus the actual position of the sign in the scene. The position is represented in this graph by means of the distance of the sign to the origin of the image (pixel (0,0) is located in the left top corner). Figure 6c points out that some correlation peaks appear in a wrong position, thus, corresponding to false alarms.

The same procedure is followed to obtain the recognition results when a second nonlinear composite filter is considered as composite nonlinear filters. Figure 7a corresponds to the probability of error in the classification of training images. We remark that the probability of error never reaches a value of zero, so that there is always a misclassification. Figure 7b shows PCE values for all the analyzed images. It can be seen that the threshold could be established only in a narrow region. We also see that the number of false alarms for non-training true targets has increased either for a PCE value under the threshold (Fig. 7b), or for the wrong location of the peak (Fig. 7c).

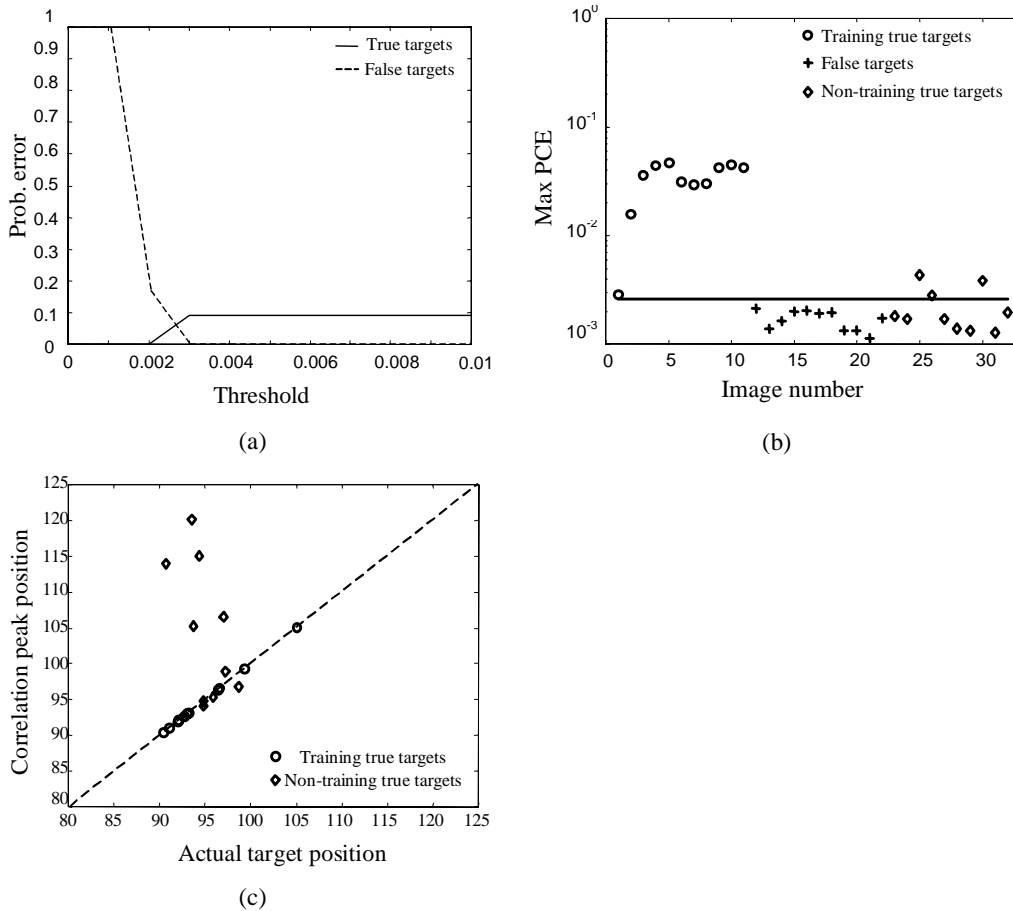


Figure 7. Recognition results for the second nonlinear composite filter. a) Probability of error in the classification of training images. b) Classification of true targets and false targets with respect to the established threshold value. c) Correlation peak position versus the actual target position in the scene.

4.3. Bank of single nonlinear filters

In the case of a filter bank, all the true target images of the training set are considered to construct a bank of single nonlinear filters. A nonlinear correlation is performed with $k=0.1$. Results are shown in figure 8. Figure 8a plots the probability of error in the classification of training images. A larger region of null probability is obtained for the filter bank than for the composite nonlinear filters used in the previous experiments. Figure 8b plots the obtained PCE values along with the established threshold. The number of misclassifications for non-training road signs is larger when composite filters rather than a filter bank are used. Nevertheless, few false alarms remain for targets located at far distances due to their low energy and resolution. Some false alarms are due to the wrong location of the correlation peak (Figure 8c).

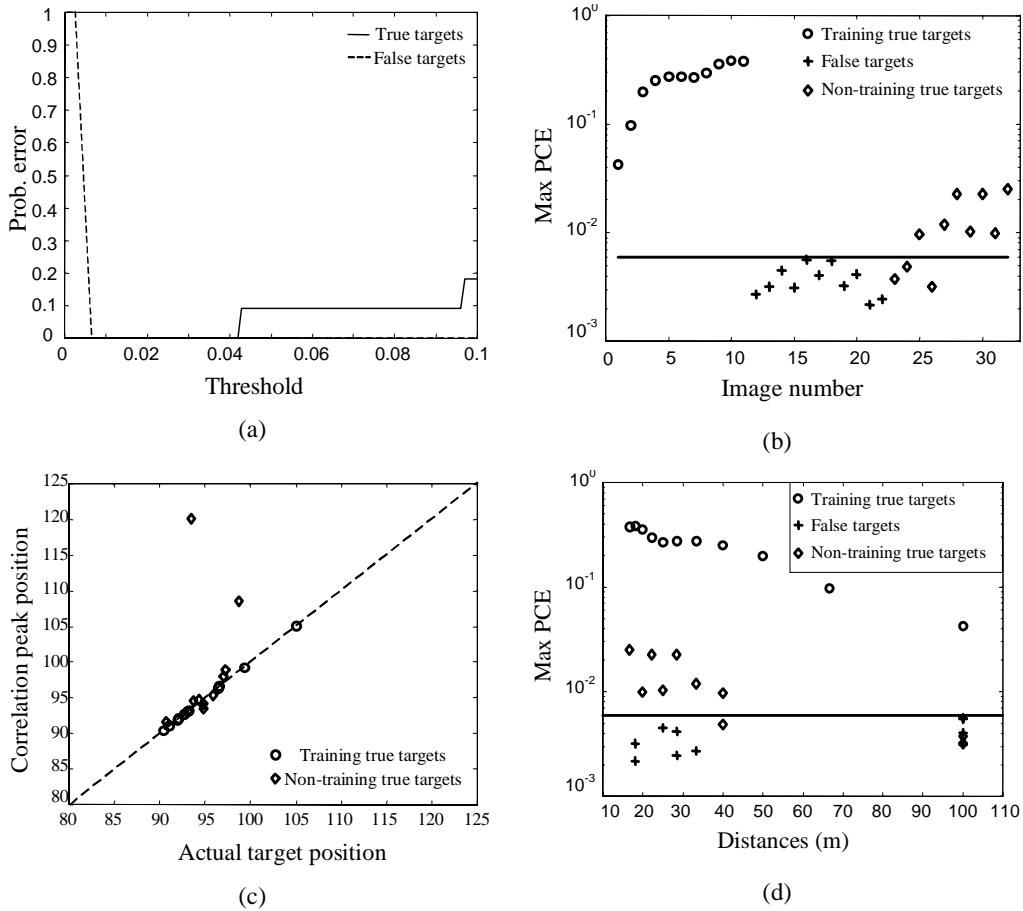


Figure 8. Recognition results for a bank of nonlinear single filters. a) Probability of error in the classification of training images. b) Classification of true targets and false targets with respect to the established threshold value. c) Correlation peak position versus the actual target position in the scene. d) maximum PCE value versus the distance between the detected road signs and the acquisition system

An advantage of using a bank of single filters is the possibility of getting more information about the detected road sign for classification or parameter estimation. For instance, the distance between the detected sign and the acquisition system will coincide approximately with the distance between the camera and the training road sign that provides the best match. This information can be easily stored in the processor. Taking into account distances between training road signs and the acquisition device,

figure 8b can be represented in the equivalent graph shown in figure 8d. Figure 8d shows the graphs of maximum PCE value versus the distance between the detected road signs and the acquisition system. In this representation, it is possible to observe that road signs at close distances are recognized. However, false alarms appear for non-training road signs captured at distances larger than 35 meters.

Obviously, the versatility of a road sign recognition system will increase if it is able to detect signs located at far distances. Not only could such a system be used in a database construction, but also as a component of a safety system installed in vehicles. The Possibility of detection of distant signs needs a limited increase in the number of training images that are at a large distances from the acquisition system. For distances larger than 30 meters, pictures are captured in intervals of 5% of scale variation. Intervals of 10% in scale are kept for short distances. A variation in the scale increment is proportional to the rate of captured frames from a video sequence at equal time intervals, provided that the vehicle has a constant velocity. Moreover, if the sign is correctly detected at far distances, we can eliminate the information of the closest road signs, and thus, reduce the number of filters in the filter bank.

Recognition results using the new bank of filters are provided in figure 9. Figure 9a corresponds to the choice of an appropriate threshold level. The learning algorithm involving a large number of training images, allows choosing a threshold level lower than the threshold value established in figure 8a.

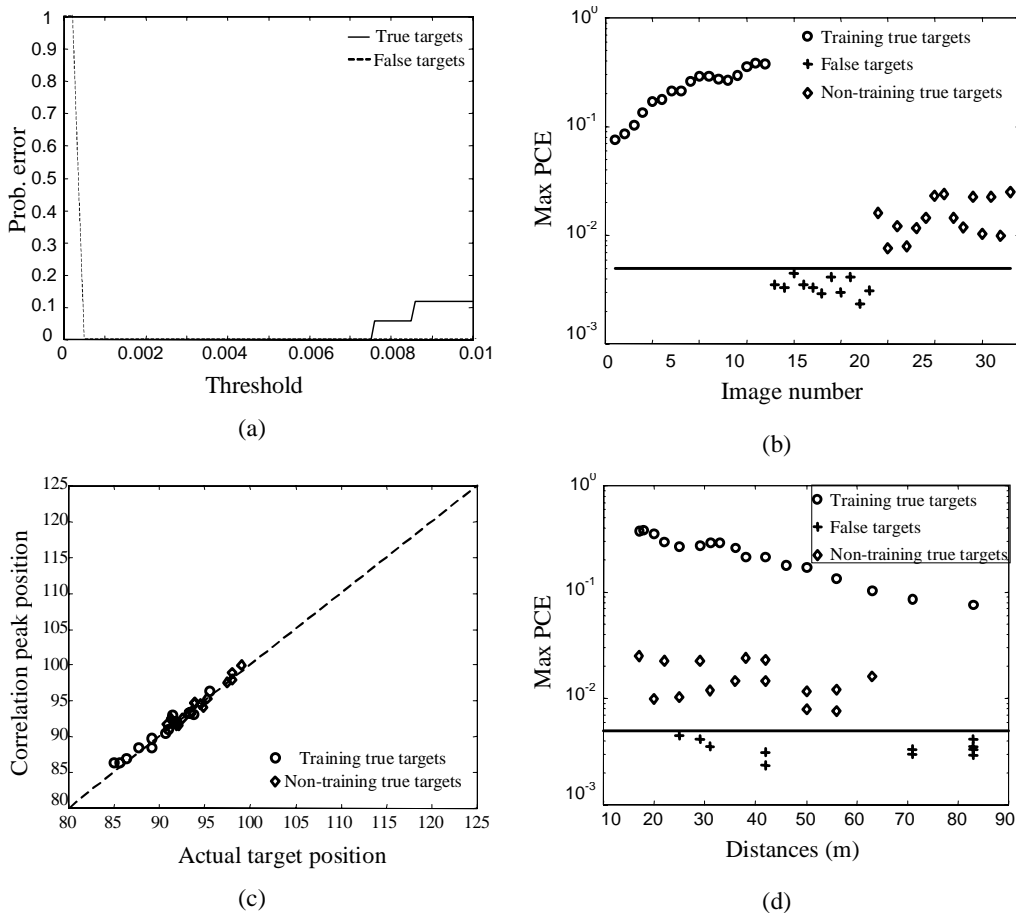


Figure 9. Recognition results for a bank of nonlinear single filters with an increase in the number of samples. a) Probability of error in the classification of training images. b) Classification of true targets and false targets with respect to the established threshold value. c) Correlation peak position versus the actual target position in the scene. d) maximum PCE value versus the distance between the detected road signs and the acquisition system

The number of non-training images in the testing set has also been increased in order to show that the recognition system is able to detect road signs located at far distances. The testing set is now

formed by 15 images captured from 18 to 60 meters away from the acquisition system, in increments of 3 meters. The recognition process is carried out for the entire set images. As shown in figures 9b and 9d, no false alarm appears among the final output results and non-training road signs are satisfactorily detected and located even for distances around 60 meters.

The experiments presented in this subsection along with results shown in the previous subsection, illustrate and compare the performance of a bank of filters and composite nonlinear filters when dealing with objects varying in scale. An increase in the number of training samples for distant targets improves the system's tolerance to scale-distortion, especially for low-resolution objects.

Nonlinear composite filters do not satisfy the requirements for discrimination capability in a scale-invariant system. These filters, however, have shown good performance when dealing with in-plane and out-of-plane versions of the target.^{6,7} One of the reasons of this behavior is that scaled images have a higher changes in energy more than rotated versions of the target.

5. ROTATION-TOLERANT ROAD SIGN RECOGNITION SYSTEM

Two types of rotation, in-plane and out-of-plane, are analyzed in this section to obtain a system tolerant to distortions.

5.1 Tolerance to out-of-plane rotations. Synthesis of composite nonlinear filters.

Taking into account all the previous results, the first recognition system was designed to identify the 35 mph speed limit sign. To achieve that, we compose nonlinear filters that include out-of-plane rotated versions of the target to be recognized. For a given distance, namely 10 m, we took out-of-plane rotated pictures of the 35 mph speed limit sign from -9 degrees to $+9$ degrees in increments of 3 step-degrees. Each element of the training set was centered in a zero background before composing the filter as showed in figure 10a. According to the analysis performed in section 4.1, we compose the nonlinear filter for a nonlinear k-value of 0.1. To accomplish scale invariance we digitally scaled all the out-of-plane-rotated images from the first training set and then we obtained 19 composites nonlinear filter, each of them is 10% percent smaller of the previous one. Four element of the filter bank are shown in figure 10b.

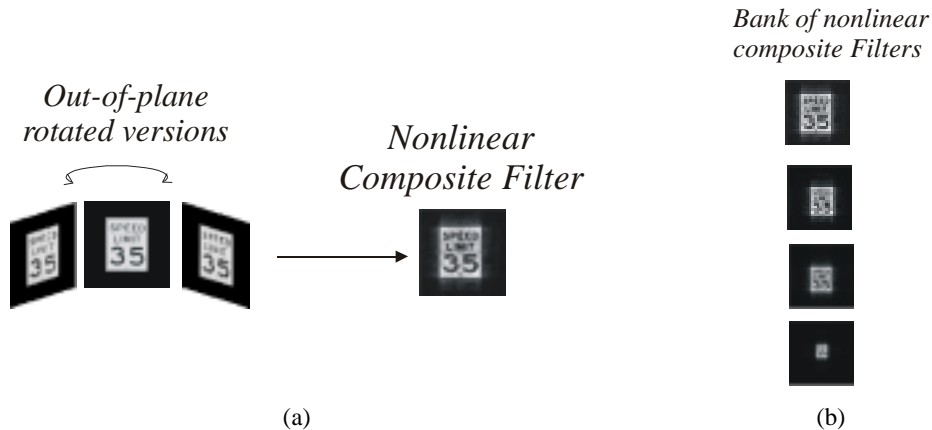


Figure 10. a) A nonlinear composite filter constructed from several out-of-plane rotated version of the 35mph speed limit sign, and b) bank of nonlinear composite filter.

5.2 Tolerance to In-Plane Rotations. Rotation of the input scene

Tolerance to in-plane rotations is achieved by rotating the input scene. A digital algorithm for rotating the signal is used to obtain in-plane rotated versions of the scene to be analyzed. We rotate the

input scene from -9 to 9 degrees in increments of 3 degrees. Rotated versions of the scene are now correlated with the nonlinear filters belonging to the bank. The output of the recognition system is related to the best match between the rotated versions of the input signal and the reference targets. Thus, the output result will correspond to the rotated scene whose correlation output has the maximum PCE value.

Figure 11 shows the distortion-tolerant system for recognizing the 35mph speed limit sign. As illustrated, the recognition system is in-plane rotation-invariant by rotating the input scene. Using composites filters that include distorted versions of the target performs the out-of-plane rotation-invariance. Moreover, since we are using a bank of composite filter, the system is scale-invariant, and as a consequence of using a nonlinear processor, the recognition system is achieving tolerance to illumination fluctuations and high discrimination capabilities under object of similar shape.

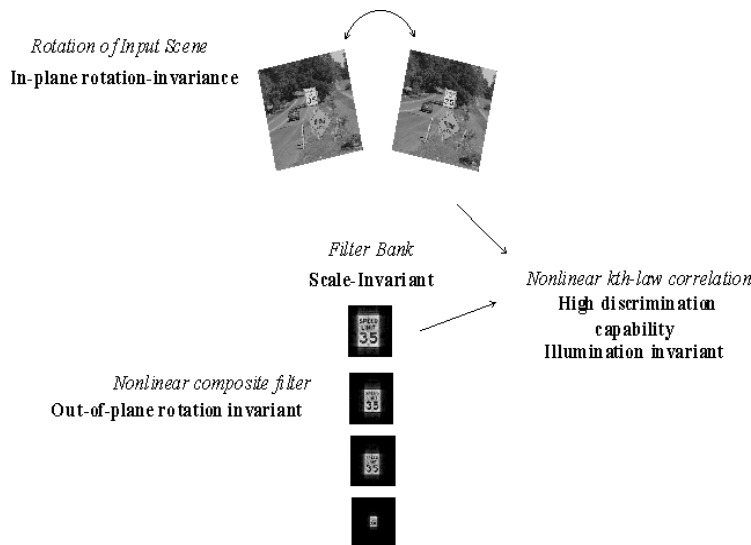


Figure 11. Recognition system for the 35mph speed limit-sign, which is tolerant to in-plane, out-of-plane rotations as well as scale and illumination-invariant.

5.3 Threshold determination

A learning algorithm allows establishing the maximum PCE value, that is the threshold value, for the recognition system. To determine the threshold value, the recognition system analyzes different images containing either true targets or false targets. The true targets set contains images with in-plane-rotated, out-of-plane rotated, near and far 35mph speed limits signs. It also contains images under poor illumination conditions. The false target set contains images of another road signs and objects similar in shape to the 35mph speed limits sign. The threshold is determined based on the results of Figure 12.

A correlation result with a PCE value greater or equal to the threshold 0.004 will result in the identification of a 35 speed limit sign in the analyzed scene. On the contrary, a PCE value smaller to the threshold will result in a rejection.

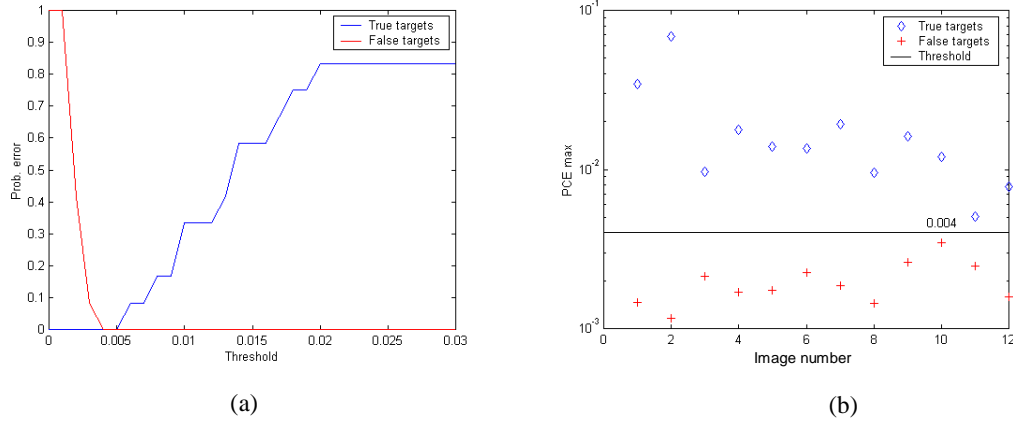


Figure 12. Determination of the threshold. a) Probability of error vs. the PCE of the correlation result; and b) PCE value for true targets and false targets.

5.4 Recognition results

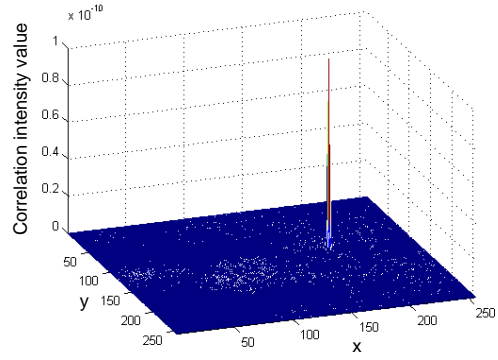
Recognition results, once the established threshold level is applied, are shown next. Recognition of the signs is always achieved by a PCE value greater than the threshold level.

Correlation peaks corresponding to the 35 speed limits signs are located at the same position as the sign in the scenes. Figure 13 shows the recognition result for a true-training speed limit sign on a real background. Figure 13a presents the analyzed scene and figure 13b shows the output correlation plane. A large and sharp correlation peak is obtained due to the perfect match between one of the filters and the training 35mph speed limits sign. Figure 13c shows the location of the detected target in the input scene.

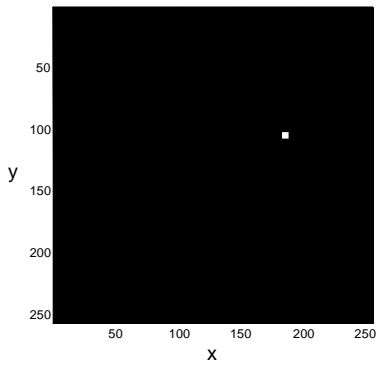
Figure 14 shows the recognition results for a true-training 35mph speed limit sign, but for a non-training scale of the road sign. It is outstanding the positive recognition of the road sign even in the presence of an object of similar shape.



(a)



(b)



(c)

Figure 13. Recognition of a true-training 35mph speed limit sign. a) Image containing a 35mph speed limit sign on a real background. b) Output correlation plane. c) Location of the detected target.

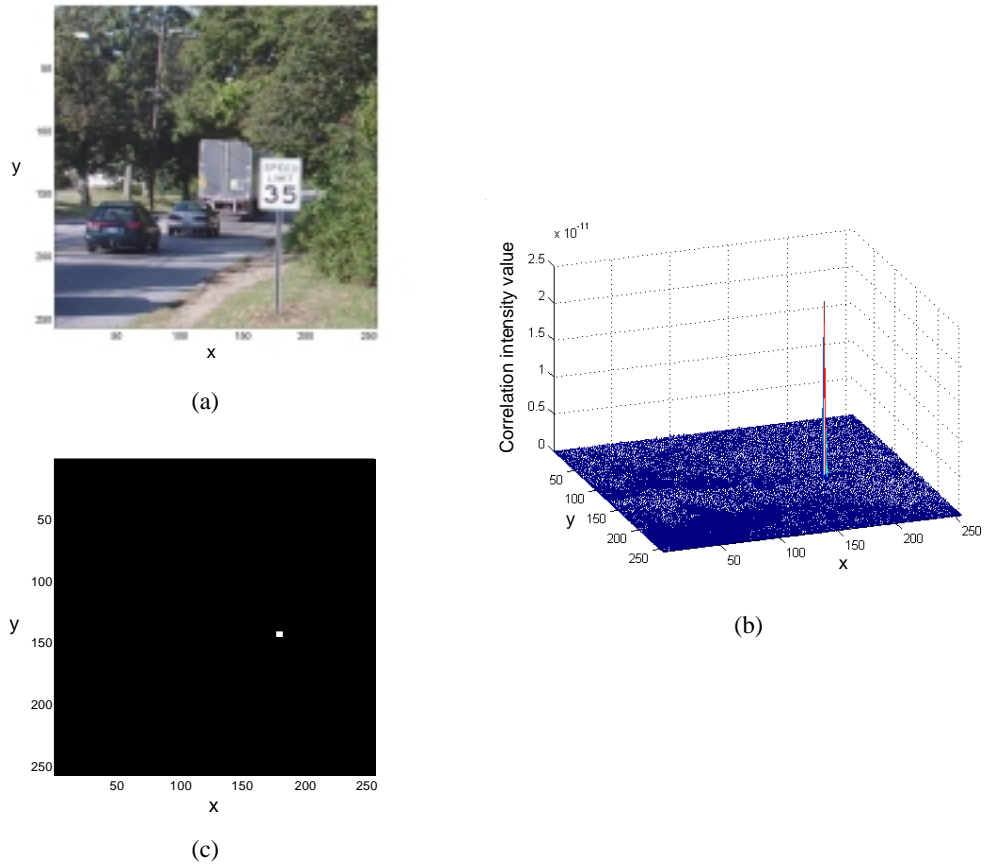


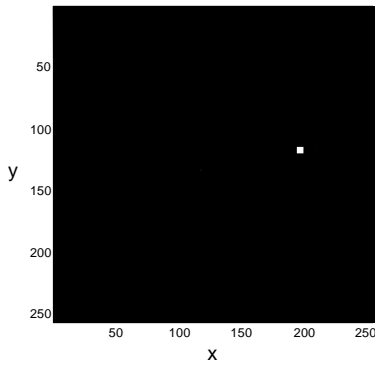
Figure 14. Recognition of training true-target for a non-training scale of the 35mph speed limit sign besides an object of similar shape. a) Analyzed scene. b) Output correlation plane. c) Location of the detected target.

The results showed in Figure 15 correspond to a non-training 35mph speed limit sign slightly in-plane rotated, in the presence of another road sign and far way from the acquisition system.

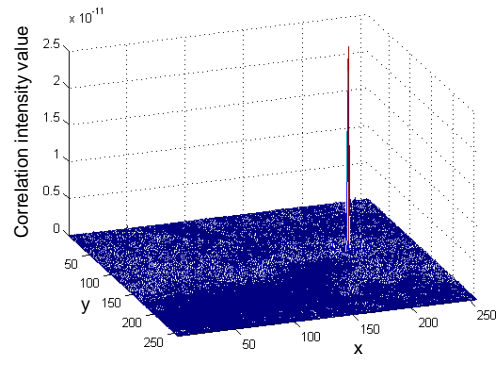
Figure 16 shows that the proposed recognition system is able to detect an out-of-plane rotated 35mph speed limit sign.



(a)



(c)



(b)

Figure 15. Identification of a far and slightly in-plane rotated 35mph speed limit sign in the presence of another road sign. a) Analyzed scene. b) Output correlation plane. c) Location of the detected target.

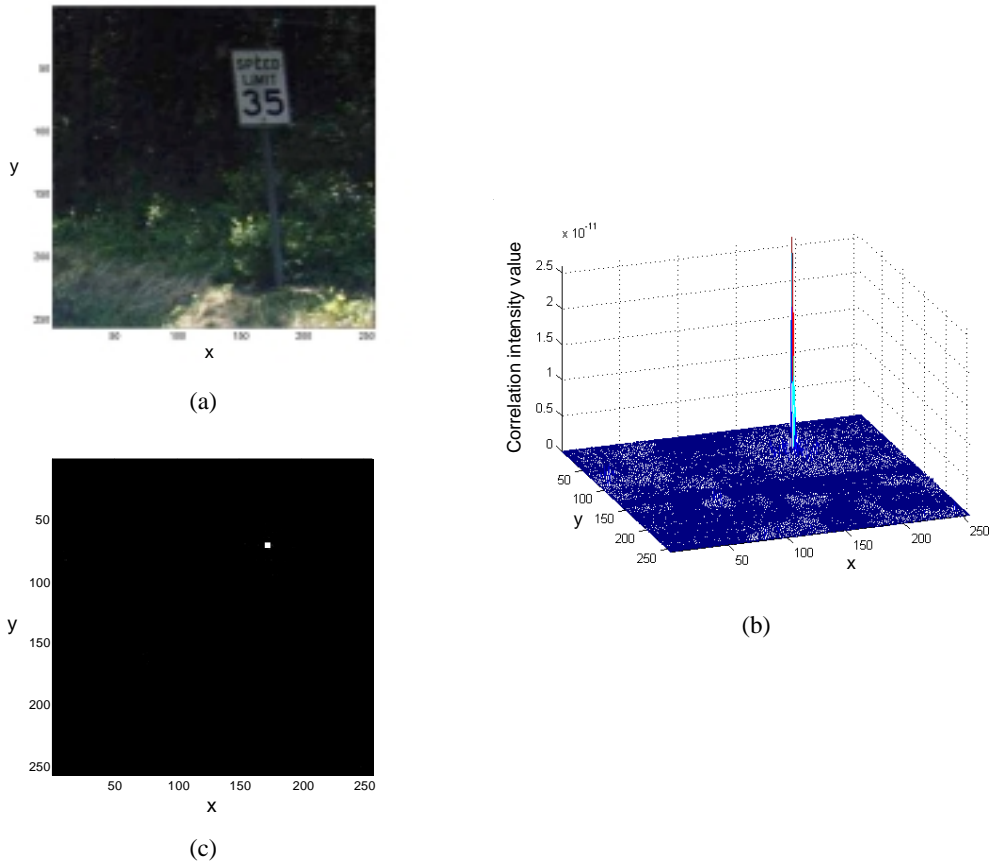


Figure 16. Identification of a rotated 35mph speed limit sign. a) Analyzed scene. b) Output correlation plane. c) Location of the detected target.

Figure 17 shows the results for a 35mph speed limit sign slightly out-of-plane rotated. Information of out-of-plane rotation is included in nonlinear composite filters and allows detecting the sign even if it is slightly out-of-plane rotated or if it is captured with a different view angle by the acquisition system.

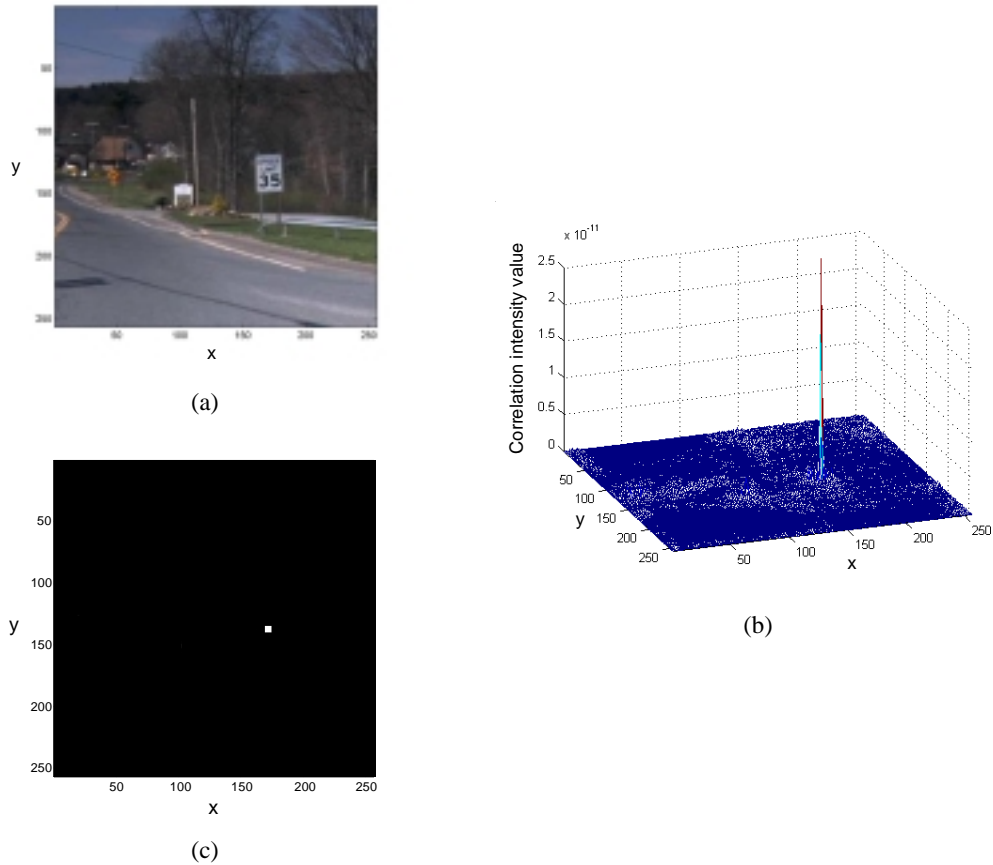
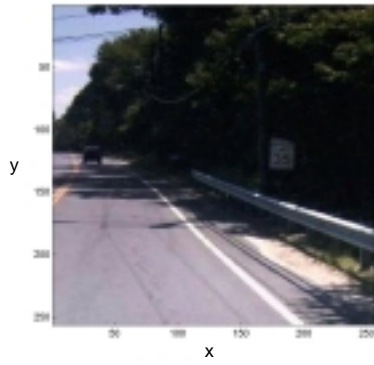
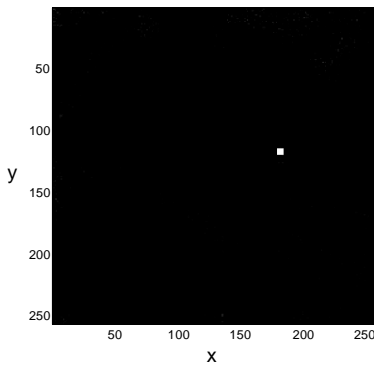


Figure 17. Out-of-plane rotated 35mph speed limits sign. a) Analyzed scene. b) Output correlation plane. c) Location of the detected target.

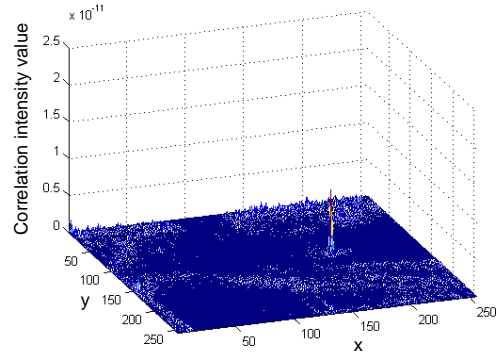
A good recognition result is the one presented in the Figure 18. The system identifies a rotated version of the target, the 35mph speed limit sign, under poor illumination. Evidently, the correlation peak showed in Fig. 18b is not as high as in the previous cases with better illuminated road signs, but it does exceed the pre-established threshold value for true target recognition. Figure 18c shows the location of the recognized speed limit sign in the input scene.



(a)



(c)



(b)

Figure 18. Recognition of a rotated true-target under poor illumination. a) Analyzed scene. b) Output correlation plane. c) Location of the detected target.

The recognition system for the 35mph speed limits sign has been proved to be very efficient identifying true targets. Now we present a couple of false targets that were rejected during the recognition process. The first one is shown in Figure 19 which corresponds to the rejection of two road signs, and figure 20 shows the rejection of a do not pass road sign.

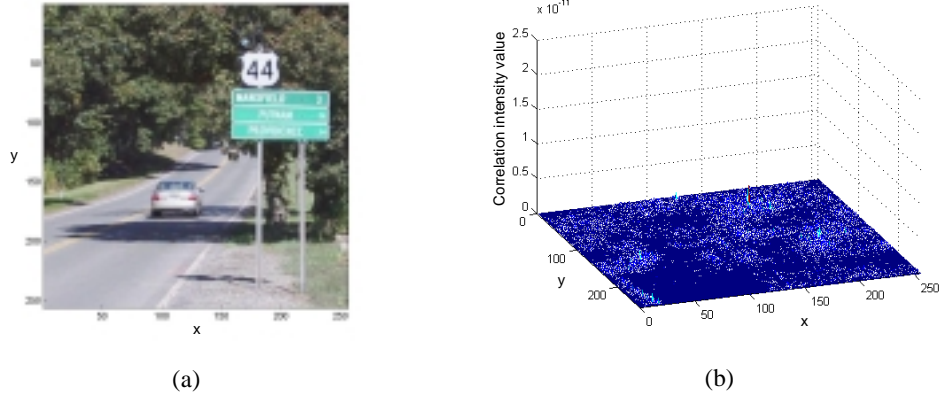


Figure 19. Rejection of a false target. a) Analyzed scene. b) Output correlation plane.

We can notice in figure 20b that a small correlation peak is located in the position of the do not pass road sign on the output correlation plane. This is mainly due to the similar shape that the speed limit sign and the do not pass sign have. This correlation peak is under the pre-established threshold so that the sign is rejected.

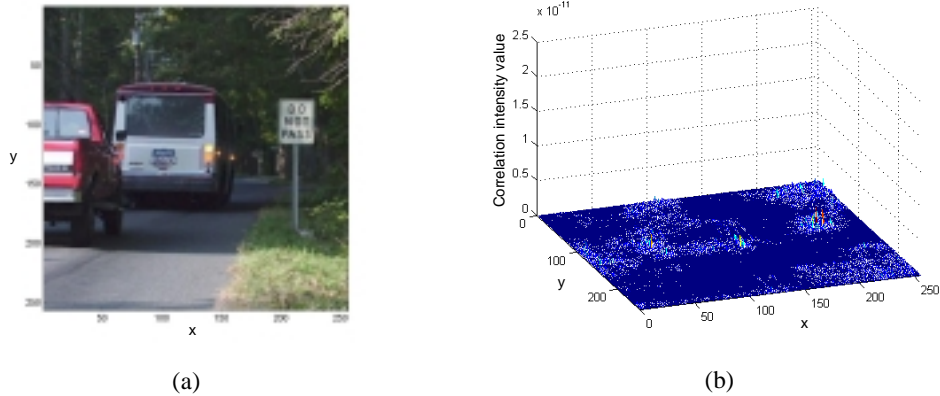


Figure 20. Rejection of a false target road sign very similar in shape to the speed limits sign. a) Analyzed scene. b) Output correlation plane.

From the result just shown, we can point out that the proposed recognition system has a high discrimination capability and thus, is able to reject signs that are quite similar in shape to the target to be recognized.

The next step is to design a recognition system that enables the detection of all the speed limit signs, that is, regardless of their speed limit number. Once the speed limit is recognized, a second step in the processor could analyze the concrete speed limit number included in the sign. In the following section we provide a description of such a system.

6. RECOGNITION SYSTEM TO DETECT ALL THE SPEED LIMIT SIGNS

In this section we present a recognition system whose goal is to identify all the speed limit road signs. The proposed system is robust to several types of distortions such as in-plane rotation, variation in scale, fluctuation in illumination, etc.

6.1 Recognition of speed limit signs regardless of their speed limit number. Synthesis of composite nonlinear filters

The recognition system is increasing in complexity since we want to recognize all the speed limit signs. One way of achieving this goal is to reproduce the same procedure of the 35mph speed limit sign recognition system now for every speed limits sign, namely 25, 30, 35, etc., but by doing that the computation time will be multiplied by the number of speed limits we want to recognize. Another option would be to build nonlinear composite filters just by keeping the shape of the speed limit sign and erasing the number in order to keep the out-of-plane rotation distortion. In this second option, problems arose due to the high similarity between the shape of the do not pass sign and the speed limit sign. In order to recognize all the speed limit signs the best trade-off between accuracy and time was accomplished by composing nonlinear filters that include all the speed limit signs for a given scale of the road sign, as showed in the figure 21.

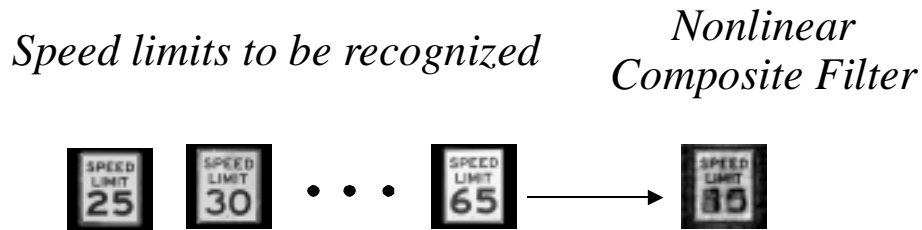


Figure 21. A nonlinear composite filter is built for comprising various speed limit signs with different speed limit number.

Again, to make the system tolerant to scale variations, we performed a digital scaling of the first training set (images taken 10 meters away from the speed limit sign) and then composing for every scale a nonlinear filter as it was explained in the previous section with the 35mph speed limit sign recognition system.

6.2 Description of the entire proposed recognition system

Figure 22 shows the proposed recognition system. The in-plane rotation-invariance was performing by rotating the input scene from -9 to +9 degrees in steps of 3 degrees. The recognition of every speed limit sign was achieved by constructing a composite filter with all the speed limit signs to be recognized. Using a bank of composite filters performed the scale-invariant-tolerant feature.

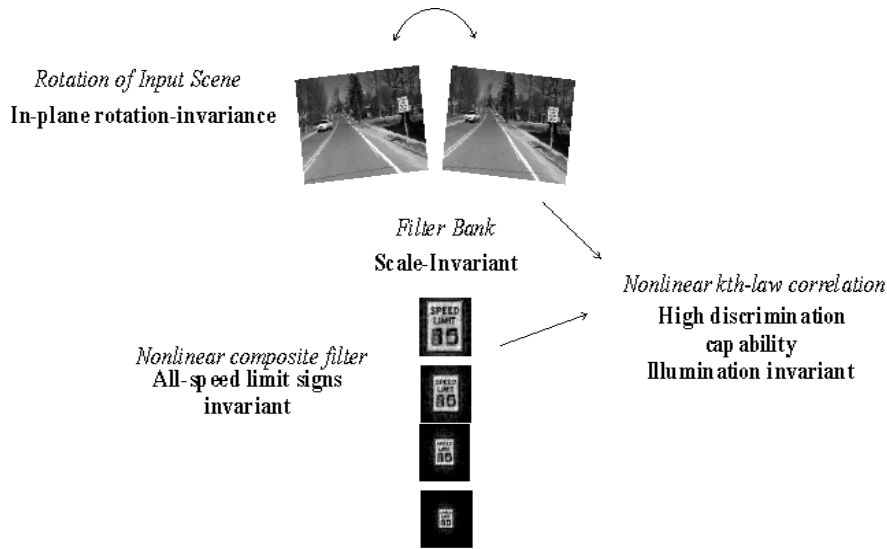


Figure 22. Recognition of all speed limit signs. System tolerant to in-plane rotations and scale-invariant. It is also robust to illumination fluctuations.

Performing a nonlinear correlation between each rotated version of the input scene and each element of the filter bank developed high discrimination capabilities. The output of the recognition system is related to the best match between the rotated versions of the input signal and the reference targets. Thus, the output result will correspond to the rotated scene whose correlation output has the maximum PCE value.

6.3 Threshold determination

As a first step, we test the entire system with the same set used for determining the threshold in the 35mph speed limit recognition system in order to compare the accuracy of the new recognition system. Figure 23 shows that for recognizing the target we have to consider a lower threshold compared to the one established for the system with the only 35mph-speed-limit filter bank. This is not a surprise, since we are removing the out-of-plane distortion tolerance feature and now we have information of another speed limits signs in the composite filter which for a particular speed limit sign could be considered as a noise, resulting in a lower peak-to-correlation energy, PCE value.

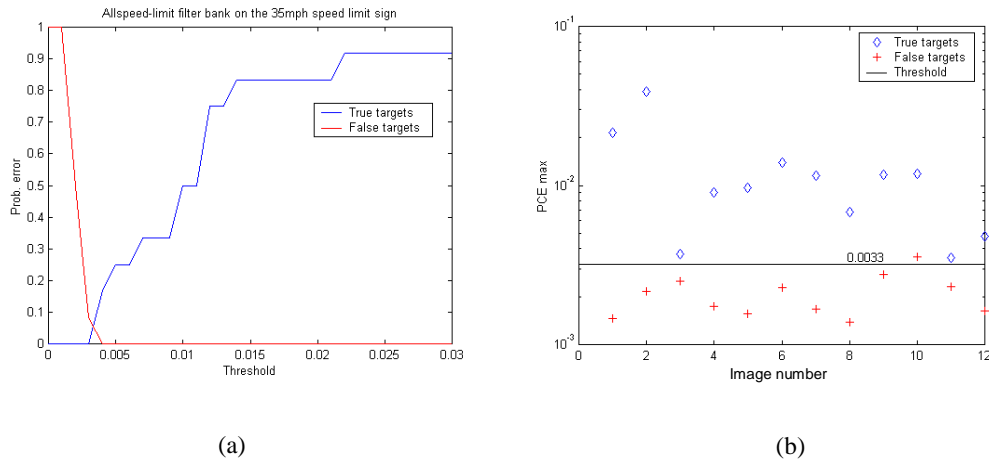


Figure 23. Determination of the threshold. a) Probability of error vs. the PCE of the correlation result; and b) PCE value for true targets and false targets.

Figure 24 shows the result of a previous example in figure 15, now using in the recognition systems the ‘all-speed limits’ nonlinear composite filter bank. The target is slightly rotated, scaled in the presence of another road sign.

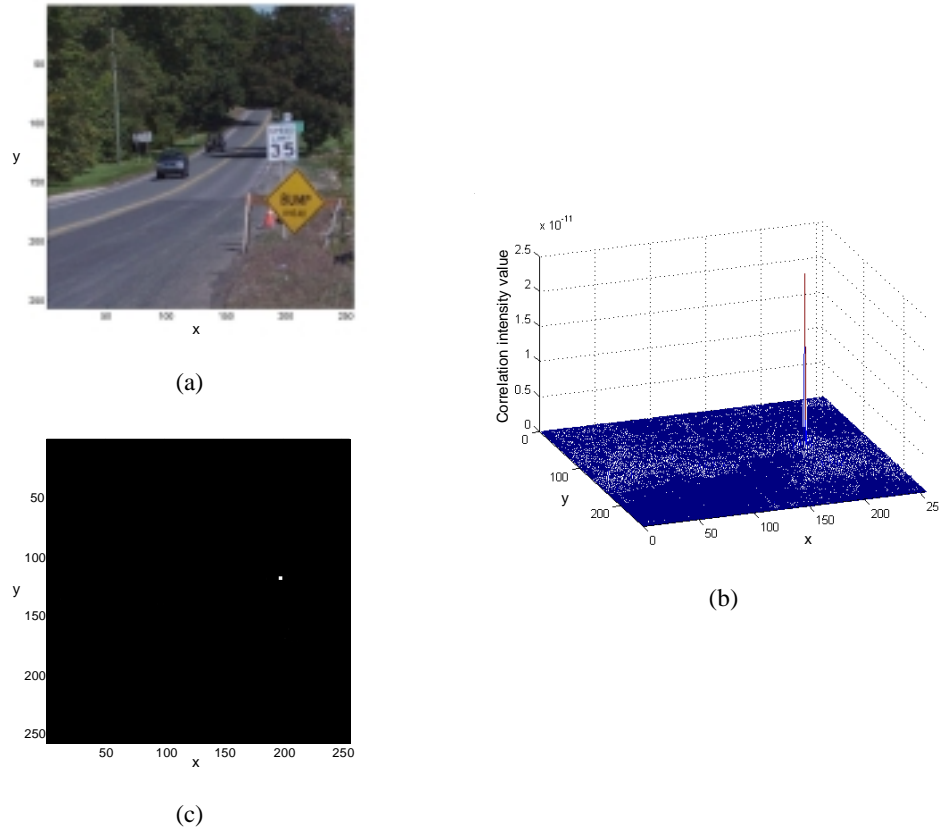


Figure 24. Results for the same image as in figure 15, now using the filter bank of nonlinear filters that comprises all the speed limits.

Now, we apply the distortion-tolerant system on images provided by the Connecticut Department of Transportation. These images were extracted from a compressed jpeg library format (.cjl). The set of images to determine the threshold includes all the speed limit signs. Figure 25 shows the results obtained while testing the recognition system with all the speed limits signs, for a variety of distortions: scale variations, poor illumination as well as rotated images. It has been shown in section 4 that one of the most critical issue in the recognition process is the scale variation so we decided to establish the threshold based on the ‘the last opportunity of detection’ for rotated and non-uniform illuminated images. Figure 26a shows the probability of error of misclassification. Figure 26b shows the PCE value for true targets and false targets.

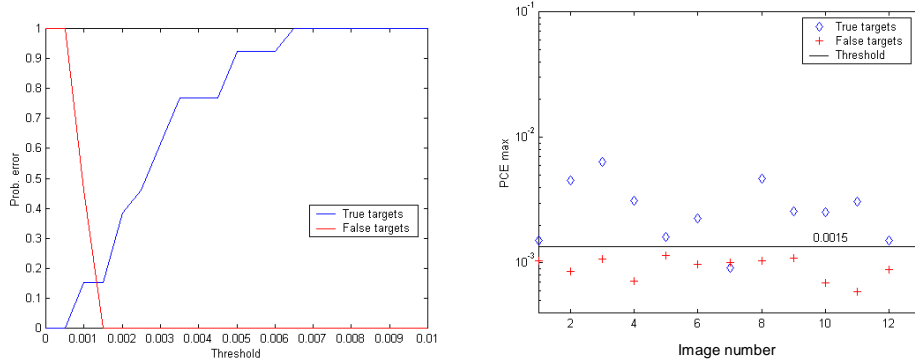


Figure 25. Probability of error using cjl images. The set of images includes different rotated, scaled and non-uniform illuminated speed limit signs.

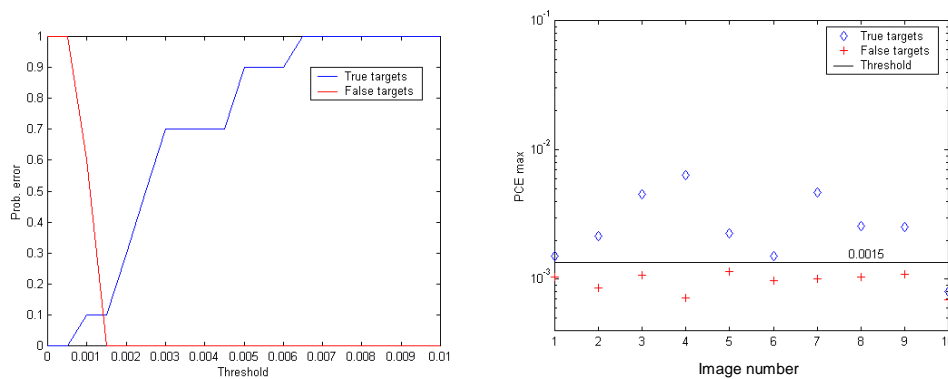


Figure 26. Threshold determination based on the ‘last opportunity of detection’ for cjl-format images.

The threshold was set on 1.5×10^{-3} . At this level, all false alarms were avoided. However, the true target image 10 will be rejected but there is nothing we can do because if we lower the threshold we are increasing the probability of accepting as true-targets the 80% of the false targets.

6.4 Recognition results

In this section we present some recognition results using the threshold previously established. A certain degree of tolerance to illumination fluctuations is achieved as a consequence of using a nonlinear processor with parameter k close to zero. Analyzed scenes were selected as samples where it is difficult to recognize the speed limit sign due to the amount of involved distortions. They are under varying illumination due to shadows or different weather conditions, and in some cases the sign to be detected appears partially occluded. In all the cases, a real cluttered background surrounds the road signs. Recognition results are presented in the following figures, where one can see the detection and location of every speed limit sign, regardless its speed limit number.

Figure 27 shows the proper detection and location of a 30mph speed limit sign in the presence of an object of similar shape included in the background. A sharp and high peak is obtained in the target position, which yields a PCE value above the established threshold.

Figure 28 shows another example of recognition of a speed limit sign along with rejection of other objects with similar energy –white cars and crosswalk –. A high and sharp peak allows detection and location of the target.

Figure 29a shows a distant 35 mph speed limit sign. The correlation plane, which is displayed as a 3D graph (Fig. 29b) and as a 2D image (Fig. 29c), points out the successful recognition of this sign despite its low resolution and non-uniform illumination.

Figure 30 present the outstanding recognition results for a 50mph speed limit sign partially occluded. The sharp and high correlation peak is achieved even though half of the sign information is occluded under poor illumination conditions.

Figure 31 presents the recognition of a non-uniform illuminated 25mph speed limit sign slightly out-of plane rotated. It is important to mention that this image was part of the threshold-determination-images set on figure 26 (image 1) and based on its PCE value we established the minimum PCE value for accepting an image as a true-target.

Figures 32-34 show other examples of recognition of 45mph, 40mph and 35mph speed limit signs.

Figure 35 presents one rejected far and non-uniform illuminated true target. The PCE of its correlation plane is lower than the pre-established threshold due to the small correlation peak in the true-position and a relative high noise due to high-energetic objects. A closer recognized-image of the same speed limit sign is presented in figure 31.

Figures 36-41 show rejection of false targets. It is remarkable the high similarity between some of these road signs and the target to be detected (speed limit signs).

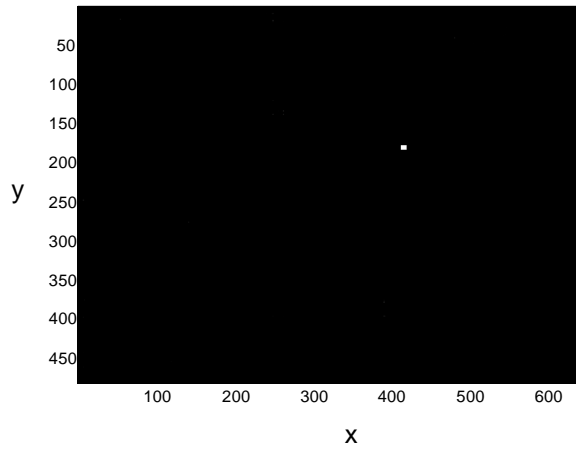
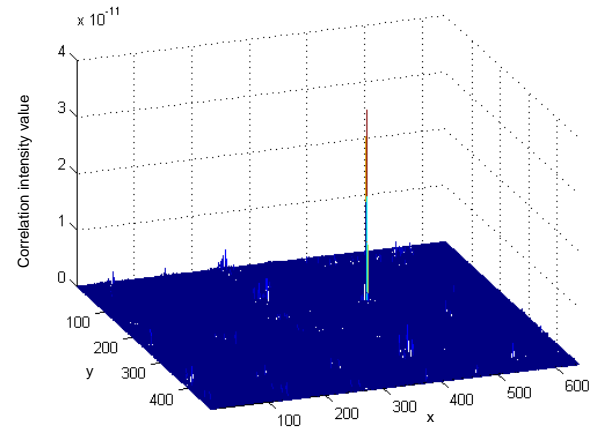
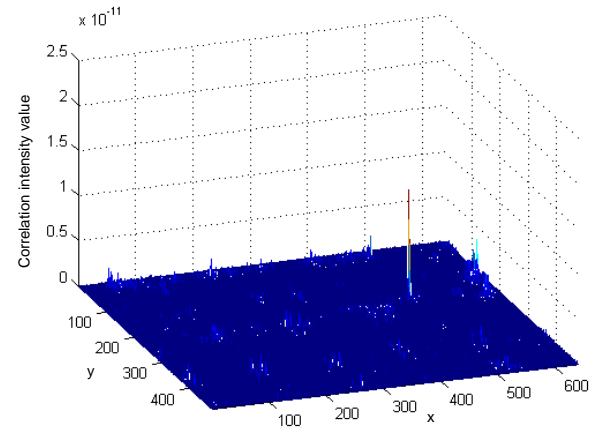


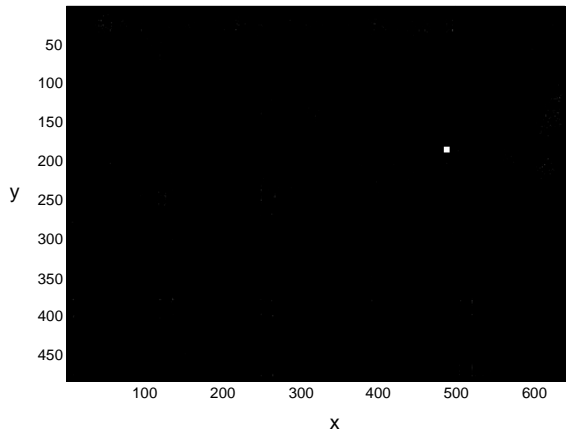
Figure 27. Detection of a slightly rotated 30mph speed limit sign in the presence of an object of similar shape. (a) Analyzed input scene. (b) Output correlation plane. (c) Location of the detected target.



(a)



(b)



(c)

Figure 29. Detection of a 35mph speed limit sign under poor illumination. (a) Analyzed input scene, (b) Output correlation plane. (c) Location of the detected target.

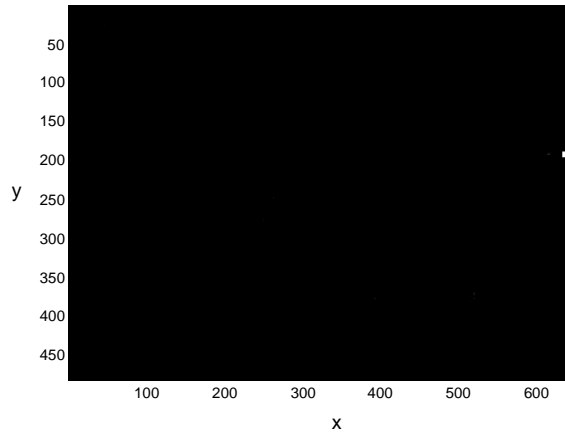
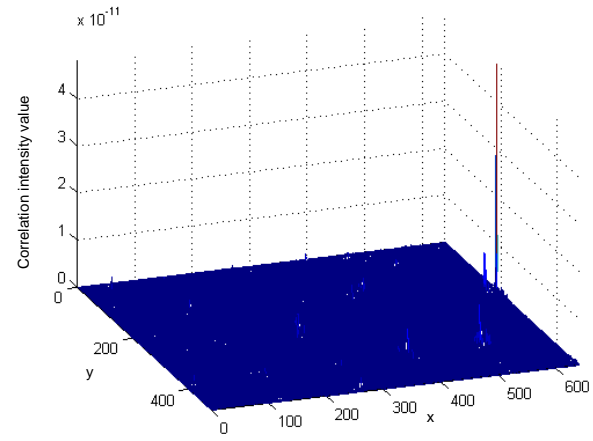
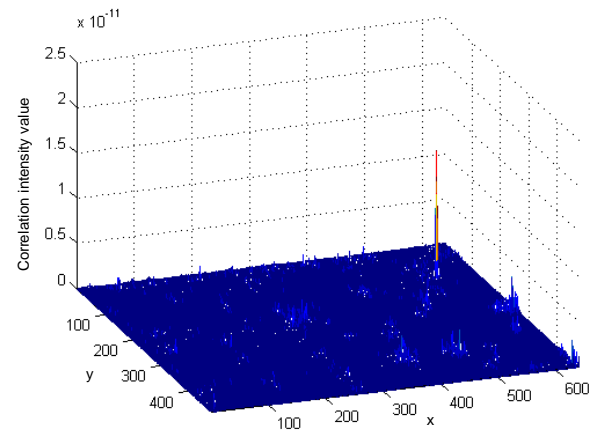


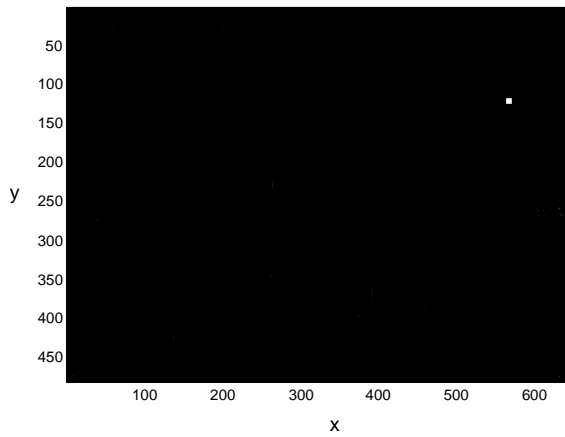
Figure 30. Recognition of a partially occluded 50mph under poor illumination. (a) Analyzed input scene. (b) Output correlation plane. (c) Location of the detected target.



(a)



(b)



(c)

Figure 31. Recognition of a 25mph speed limit sign under non-uniform illumination. (a) Analyzed input scene. (b) Output correlation plane. (c) Location of the detected target.

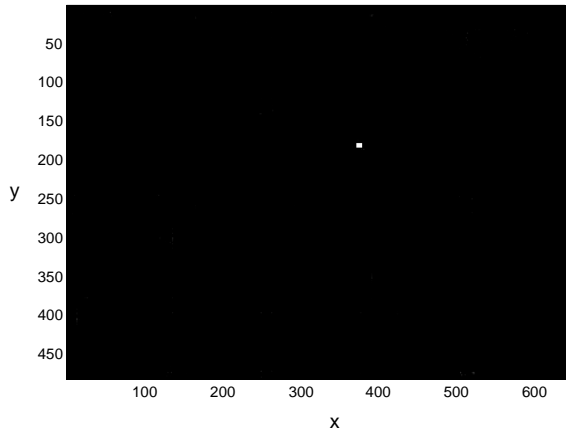
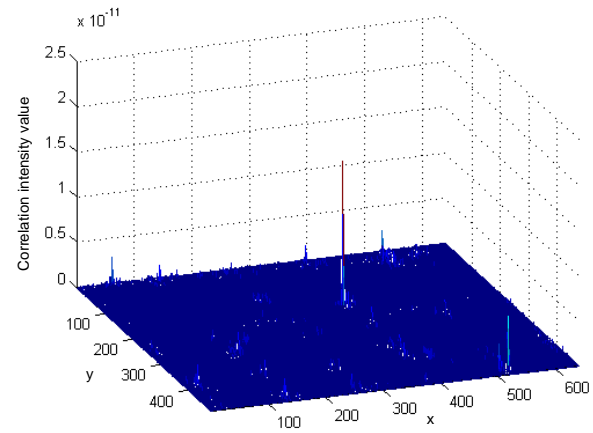
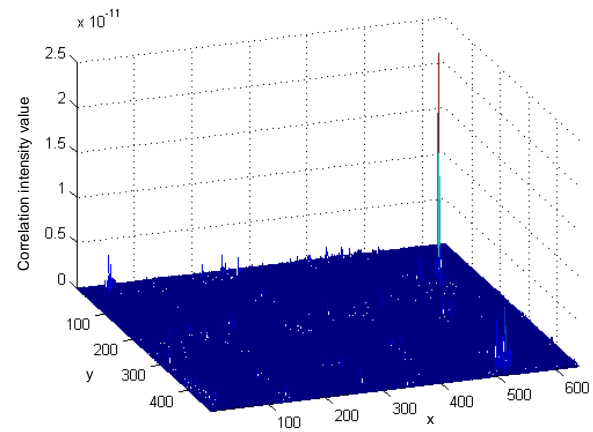


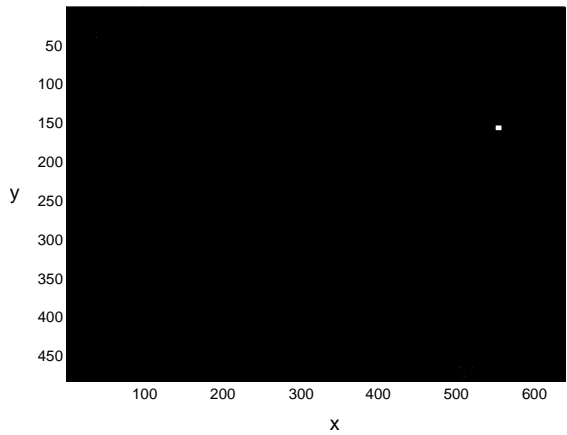
Figure 32. Recognition of a far slightly rotated 45mph speed limit sign in the presence of another road sign. (a) Analyzed input scene. (b) Output correlation plane. (c) Location of the detected target.



(a)



(b)

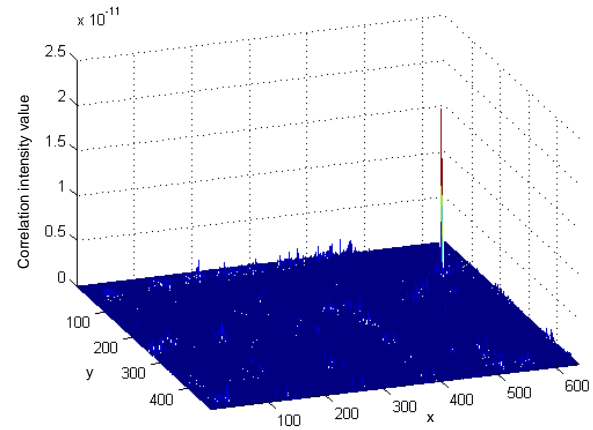


(c)

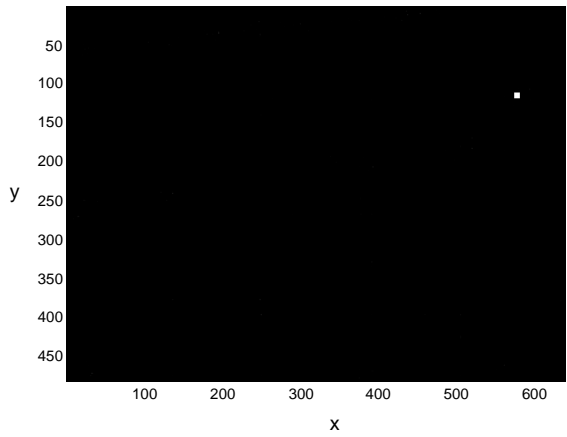
Figure 33. Recognition of a 40mph speed limit sign in the presence of a highly energetic demarcation line. (a)Analyzed input scene. (b) Output correlation plane. (c) Location of the detected target.



(a)



(b)

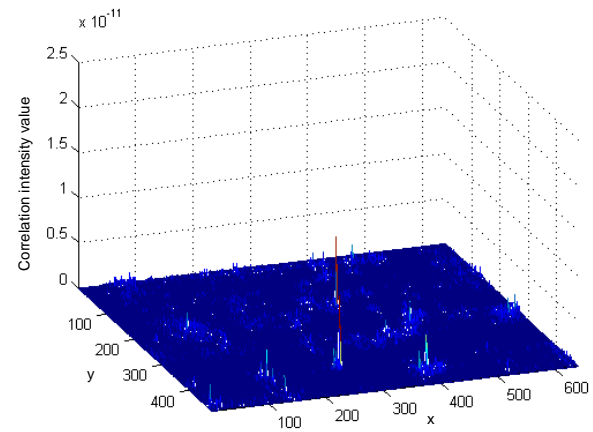


(c)

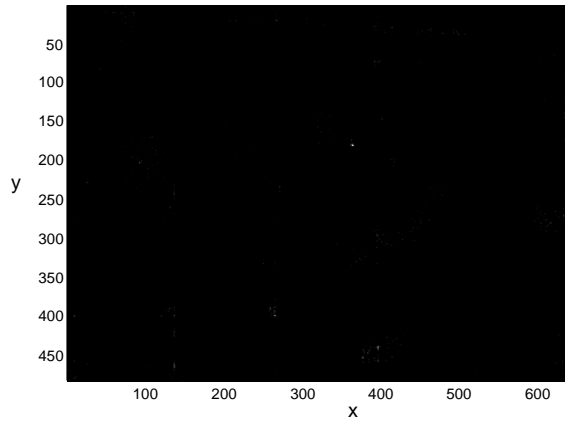
Figure 34. Recognition of a rotated 35mph speed limit sign. (a) Analyzed input scene. (b) Output correlation plane. (c) Location of the detected target.



(a)



(b)

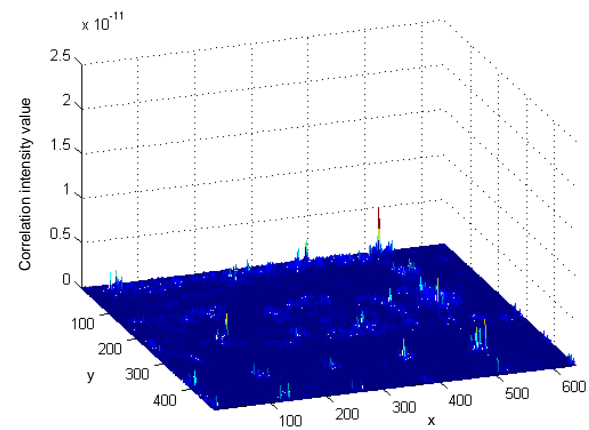


(c)

Figure 35. Rejection of a far and non-uniform illuminated true target. The PCE of this correlation plane is lower than the pre-established threshold due to the small correlation peak in the true-position and a relative high noise due to other energetic objects. A closer recognized-image is presented in figure 31. (a) Analyzed input scene. (b) Output correlation plane. (c) Location of the detected target.



(a)

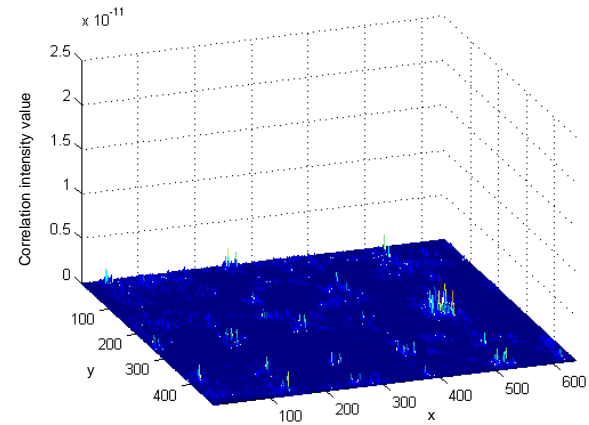


(b)

Figure 36. Rejection of false targets. Several road signs are present in the scene. (a) Analyzed input scene, (b) Output correlation plane.



(a)



(b)

Figure 37. Rejection of a false target of similar shape (a) Analyzed scene (b) Output correlation plane.

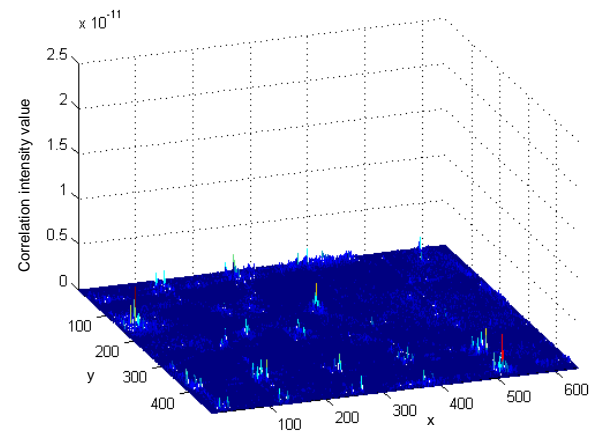
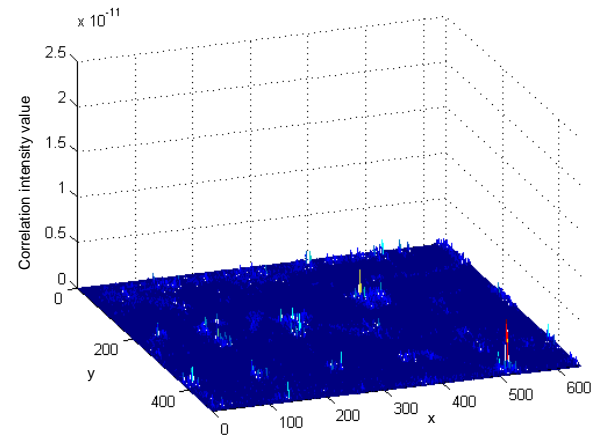


Figure 39. Rejection of a false target. (a) Analyzed scene. (b) Output correlation plane.



(a)

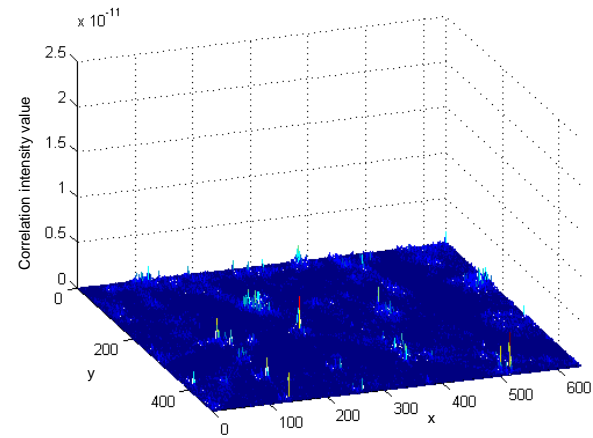


(b)

Figure 40. Rejection of a false target. (a) Analyzed scene. (b) Output correlation plane.



(a)



(b)

Figure 41. Rejection of a false target. (a) Analyzed scene. (b) Output correlation plane.

7. ANALYSIS OF A VIDEO SEQUENCE

To sum up all the experiments carried out in the design of a scale, rotation and illumination-invariant recognition system, a video sequence of a speed limit sign was registered. Images displayed in figure 42 are extracted from this video sequence. They show a speed limit sign increasing in scale as the vehicle was in motion. They are under non-uniform illumination. The corresponding correlation outputs are also shown in this figure, next to each image. In all the cases, a sharp peak is projected over a low energy background. The location of the peak corresponds in all the cases to the position of the road sign in the analyzed image.

The positive recognition of the road sign included in this video sequence allows us to post-process these results to obtain a unique identification of the same speed limit sign with a reduced probability of error. Moreover, it allows tracking the position of a detected target through a sequence of images.

8. SUMMARY

A road sign recognition system has been proposed based on nonlinear processors. The analysis of different filtering methods allows us to select the best techniques to overcome a variety of distortions. The most frequent distortions when dealing with road sign detection are scale variations, in-plane and out-of-plane rotation and illumination variations of the targets.

The entire processor performs several correlations between different input scenes and a set of reference targets. Multiple correlation results are then processed to give a single recognition output. A learning process is carried out to establish a threshold value, which determines whether or not any object contained in an input scene is similar to the target.

Scale-invariance is provided to the recognition system by means of a bank of nonlinear filters. A filter bank recognition system shows a better performance than nonlinear composite filters. Images of a true target captured from different speed limit signs constitute the set for one composite filter. A bank of nonlinear composite filters was built from digitally scaled versions of the captured images. A non-uniform increment of variation in scale is established to properly recognize signs located at far distances from the acquisition system.

In-plane rotation invariance is achieved by rotating the input scene. Recognition results obtained by this method are compared to results obtained for nonlinear composite filters. Composite filters are constructed by using digital rotated versions of the reference target for one specific speed limit sign (35mph). In-plane rotation of the input scene allows better detection results than composite filters. Moreover, in the design of composite filters the maximum number of images included in a composite filter is limited, whereas the range of the input scene rotation can be determined based on the application

Using nonlinear composite filters rather than using individual filters in the filter bank can satisfy the tolerance requirements for out-of-plane rotation of the targets. In particular, nonlinear ECP SDF and nonlinear MACE filters are used.

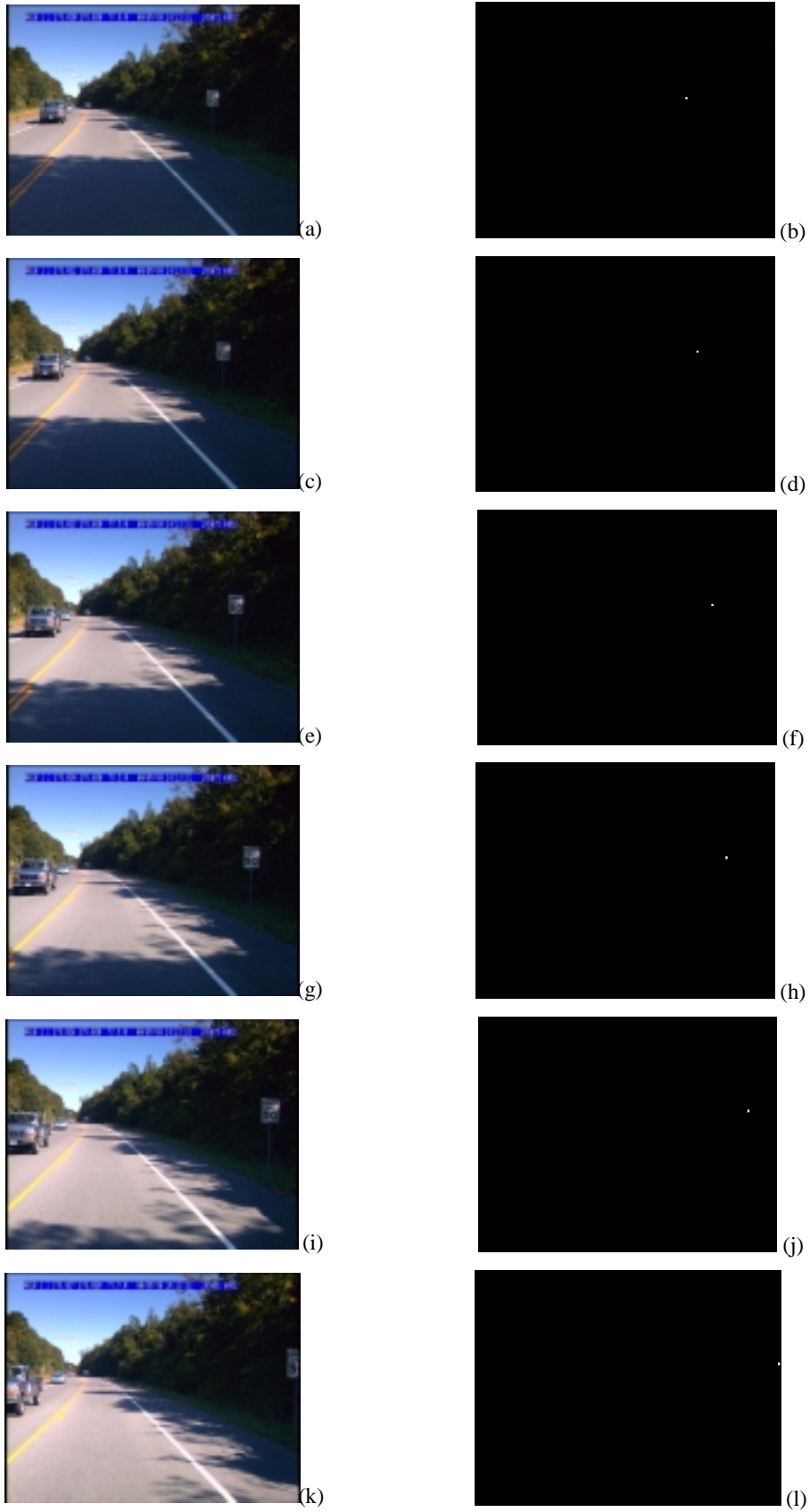


Figure 42. Recognition results for the analysis of a video sequence.

The entire recognition system has been tested in real still images as well as in a video sequence. Scenes were captured in real environments, with cluttered backgrounds and contained many distortions simultaneously. Recognition results for various images show that, the proposed recognition system is able to properly detect a given road sign even if it is varying in scale, slightly tilted or viewed under different angles. In addition, the system is robust to changes in illumination due to shadows or weather conditions. It is also able to locate a faded or vandalized sign along with partially occluded road signs. Obviously, the processor can be designed for different varieties of road signs in noisy background scenes.

As a further research, the system should be applied to a large set of images encompassing most situations encountered in an operational setting. This would provide a rigorous test of the system capability and it would be possible to evaluate its accuracy.

REFERENCES

1. H. J. Caulfield, W. T. Maloney, "Improved discrimination in optical character recognition," *Appl. Opt.*, 8 (11), 2354-2356 (1969).
2. H. J. Caulfield, "Linear combinations of filters for character recognition: a unified treatment," *Appl. Opt.*, 19, 3877-3879 (1980).
3. C. F. Hester, D. Casasent, "Multivariate technique for multiclass pattern recognition," *Appl. Opt.*, 19 (11), 1758-1761 (1980).
4. D. Casasent, "Unified synthetic discriminant function computational formulation," *Appl. Opt.*, 23 (10), 1620-1627 (1984).
5. A. Mahalanobis, B. V. K. Vijaya Kumar, D. Casasent, "Minimum average correlation energy filters," *Appl. Opt.*, 26 (17), 3633-3640 (1987).
6. B. Javidi, D. Painchaud, "Distortion-invariant pattern recognition with Fourier-plane nonlinear filters," *Appl. Opt.*, 35 (2), 318-331 (1996).
7. B. Javidi, W. Wang, G. Zhang, "Composite Fourier-plane nonlinear filter for distortion-invariant pattern recognition," *Opt. Eng.*, 36 (10), 2690-2696 (1997).
8. B. Javidi, J. L. Horner, A. Fazlollahi, J. Li, "Illumination-invariant pattern recognition with a binary nonlinear joint transform correlator using spatial frequency dependent threshold function," in *Proc. SPIE*, 2026, 100-106 (1993).
9. E. Silvera, T. Kotzer, J. Shamir, "Adaptive pattern recognition with rotation, scale, and shift invariance," *Appl. Opt.*, 34 (11), 1891-1900 (1995).
10. Ph. Réfrégier, B. Javidi, G. Zhang, "Minimum mean-square-error filter for pattern recognition with spatially disjoint signal and scene noise," *Opt. Lett.*, 18 (17), 1453-1455 (1993).
11. Ph. Réfrégier, V. Laude, B. Javidi, "Nonlinear joint-transform correlation: an optimal solution for adaptive image discrimination and input noise robustness," *Opt. Lett.*, 19 (6), 405-407 (1994).
12. B. Javidi, J. Wang, "Optimum distortion-invariant filter for detecting a noisy distorted target in nonoverlapping background noise," *J. Opt. Soc. Am. A*, 12 (12), 2604-2614 (1995).
13. B. Noharet, R. Hey, H. Sjöberg, "Comparison of the performance of correlation filters on images with real-world non-overlapping noise: influence of the target size, illumination and in-plane rotation distortion," in *Proc. SPIE*, 3386, 212-221 (1998).
14. L. Guibert, G. Keryer, A. Serval, M. Attia, H. S. MacKenzie, P. Pellat-Finet, J. L. de Bougrenet de la Tocnaye, "On-board optical joint transform correlator for real-time road sign recognition," *Opt. Eng.*, 34 (1), 135-143 (1995).

15. T. D. Wilkinson, Y. Perillot, R. J. Mears, J. L. de Bougrenet de la Tocnaye, "Scale-invariant optical correlators using ferroelectric liquid-crystal spatial-light modulators," *Appl. Opt.*, 34 (11), 1885-1890 (1995).
16. M. Taniguchi, K. Matsuoka, "Detection of road signs by using a multiple correlator and partial invariant filters," *Proc. SPIE*, 3490, 178-181 (1998).
17. M. Taniguchi, Y. Mokuno, K. Kintaba, K. Matsuoka, "Correlation filter design for classification of road sign by multiple optical correlators," *Proc. SPIE*, 3804, 140-147 (1999).
18. J. W. Goodman, "Introduction to Fourier Optics," 2nd ed. New York: McGraw-Hill (1996).
19. J. D. Gaskill, "Linear systems, Fourier transforms, and optics," John Wiley & Sons, New York (1987).
20. A. B. Vander Lugt, "Signal detection by complex filtering," *IEEE Trans on Inf. Theory*, IT-10, 139-145 (1964).
21. J. Campos, F. Turon, L. P. Yaroslavsky, M. J. Yzuel, "Some filters for reliable recognition and localization of objects by optical correlators: a comparison," *Int. J. Opt. Comp.*, 2, 341-365 (1991).
22. O. K. Ersoy, M. Zeng, "Nonlinear matched filtering," *J. Opt. Soc. Am., A*, 6 (5), 636-648 (1989).
23. B. Javidi, "Generalization of the linear matched filter concept to nonlinear matched filters," *Appl. Opt.*, 29 (8), 1215-1224 (1990).
24. Ph. Réfrégier, "Filter design for optical pattern recognition: multicriteria optimization approach," *Opt. Lett.*, 15 (15), 854-856 (1990).
25. Ph. Réfrégier, "Optimal trade-off filters for noise robustness, sharpness of the correlation peak, and Horner efficiency," *Opt. Lett.*, 16 (11), 829-831 (1991).
26. B. Javidi, "Nonlinear joint power spectrum based optical correlation," *Appl. Opt.*, 28 (12), 2358-2367 (1989).
27. J. L. Horner, "Metrics for assessing pattern-recognition performance," *Appl. Opt.*, 31, 165-166 (1992).